CHARACTERIZING THE NOVEL INTERACTION BETWEEN HUMAN UBIQUITIN SPECIFIC PROTEASE 7 (USP7) AND FORKHEAD BOX M1 (FOXM1)

ANEESAH MALIK

A THESIS SUBMITTED TO THE FACULTY OF GRADUATE STUDIES IN PARTIAL FULFILMENT OF THE REQUIREMENTS FOR THE DEGREE OF

MASTER OF SCIENCE

GRADUATE PROGRAM IN BIOLOGY

YORK UNIVERSITY

TORONTO, ONTARIO

JUNE 2022

ABSTRACT

Ubiquitin Specific Protease 7 (USP7) is a deubiquitinase that cleaves ubiquitin from substrate protein(s) in order to alter their stability, localization or activity. USP7 is essential as it regulates the stability of many proteins involved in various cellular pathways. USP7 utilises the ^{164}DWGF^{167} motif found in the TRAF domain at the NTD of USP7 to interact with substrates containing P/A/ExxS motifs. Many P/A/ExxS motifs were identified in Forkhead Box M1 (FOXM1), a transcription factor whose expression is exclusively found in cells that are actively proliferating, and is responsible for activating transcription of genes needed for cell cycle progression. Pull-down assays demonstrated that USP7 and FOXM1 interact *in vivo*, and *in vitro*. FOXM1 levels were shown to vary depending on the amount of USP7 present *in vivo*, indicating that USP7 regulates FOXM1 stability. As a result, FOXM1 has been identified as a novel interacting partner of USP7.

ACKNOWLEDGEMENTS

I would like to thank my supervisor, Dr. Vivian Saridakis, for the opportunity to conduct my graduate research in her lab. I will always be grateful for all of the insightful conversations we had. It was definitely tough doing my master's in the midst of a pandemic, and I could not have asked for a better supervisor to guide me.

Thank you to Dr. Michael Scheid, my advisor, your perceptive questions during my committee meetings provided me with a different perspective on my project, allowing me to consider possibilities I hadn't before. The advice you provided was constructive and helped me succeed.

Thank you to the members of the Saridakis lab, Anna, Helen, Sukhdeep and Krstina. Anna, and Helen thank you for teaching me crucial lab techniques that I used throughout my master's. Sukhdeep and Krstina, thank you for always being there, and for making me laugh every day in the lab.

Thank you to David, Jennifer, Marjaan, Farnaz, Nick, Kyra, and the many graduate students I met during my time at LSB. Thank you for your consistent support, the advice you provided, and for answering my questions.

To my incredible family, thank you for supporting me. Mom, and Dad, your unwavering belief in my ability to succeed even when I didn't believe in myself was precisely what I needed to remain motivated. Umair, no one else would have put up with me for so long, thank you. Rabiah, my life became more enjoyable when you came into it, thank you. Thank you to Hafsaah for your constant support, and for always being there for me. Amna, thank you for being a great friend. You are all immensely important to me, and have helped shape who I am, thank you.

TABLE OF CONTENTS

LIST OF TABLES

LIST OF FIGURES

LIST OF ABBREVIATIONS

Amino-Terminal Domain	NTD
Adenomatous Polyposis Coli	APC
Anaphase Promoting Complex/Cyclosome	APC/C
Autism Spectrum Disorder	ASD
Adenosine triphosphate	ATP
β-transducin Repeats-Containing Proteins	β-TrCP
β-catenin inhibitory domain	CID
Budding Uninhibited by Benzimidazoles 3 homolog	Bub3
Casein Kinase 1	CK1
Catalytic Domain	CAT
Carboxy-Terminal Domain	CTD
Centromere Protein F	CENP-F
Checkpoint with Forkhead and Ring Finger Domains	CHFR
CREB Binding Protein	CBP
Cyclin dependent kinase	Cdk
Deubiquitinase	DUB
Deoxyribonucleic acid	DNA
DNA Binding Domain	DBD
Enhancer of Zest Homolog 2	EZH2
Epstein-Barr Virus	EBV
Epstein-Barr Virus Nuclear Antigen 1	EBNA1
F-box Only Protein 38	FBXO38
F-Box and WD Repeat Domain Containing 7	FBXW7

Forkhead	FKH
Forkhead box M1	FOXM1
Glycogen Synthase Kinase 3	GSK3
Herpesvirus-Associated Ubiquitin-Specific Protease	HAUSP
Herpes Simplex Virus HSV-1 Protein Infected Cell Protein 0	ICP0
Homologous to the E6AP Carboxyl (C) Terminus	HECT
I-kappa B Kinase complex	IKK
Inhibitor of β-catenin and TCF4	ICAT
JAB1/MPN/MOV34 Metalloprotease	JAMM
Kaposi's Sarcoma Herpesvirus	KSHV
kiloDalton	kDa
Kinesin Family Member 20A	KIF20A
Kinesin Family Member 20B	KIF20B
Lymphoid Enhancer Factor	LEF
Machado-Joseph Domain Protease	MJD
Meprin and Traf Homology	MATH
Mitogen-Activated Protein	MAP
Motif Interacting with Ubiquitin (MIU)- containing Novel DUB Family	MINDY
Mouse Double Minute 2 Homolog	MDM2
N-terminal Methionine	M1
Negative Regulatory Domain	NRD
Ovarian Tumour Related Proteases	OUT
Pancreatic Ductal Adenocarcinoma	PDA
Polo-like kinase 1	Plk1

Proliferating Cell Nuclear Antigen	PCNA
Ubiquitin Binding Domain	UBD
Ubiquitin C-terminal Hydrolases	UCH
Ubiquitin Like	Ubl
Ubiquitin Specific Protease	USP
Ubiquitin Specific Protease 5	USP5
Ubiquitin Specific Protease 7	USP7
Ubiquitin Specific Protease 21	USP21
Ubiquitin Specific Protease 22	USP22
Ubiquitin Specific Protease 28	USP28
Ubiquitin-like with PHD And Ring Finger Domains 1	UHRF1
Ubiquitin Proteasome System	UPS
Really Interesting New Gene	RING
Receptor associated protein 80	Rap80
Retinoblastoma-associated protein	Rb
RING-between- RING	RBR
Ring Finger Protein 220	RNF220
S-phase kinase-associated protein 2	Skp2
Short hairpin FOXM1	shFOXM1
Spindle Assembly Checkpoint	SAC
T-cell factor	TCF
T-cell factor 4	TCF4
TCF binding element	TBE
Transactivation Domain	TAD

Transforming growth factor β Activated Kinase-1	TAK1
Tumor Necrosis Factor Receptor-Associated Factor	TRAF
Vascular Endothelial Growth Factor	VEGF
Wnt responsive elements	WRE
Zinc	Zn
Zinc Finger MIZ-Type Containing 2	ZMIZ2

CHAPTER 1: INTRODUCTION

1.1 Ubiquitination

Ubiquitination is a reversible post-translational modification of proteins mediated by enzymatic processes that result in the covalent attachment of evolutionarily conserved ubiquitin, a 76 amino acid residue polypeptide, to a lysine (K) residue on the substrate protein (Chan & Hill, 2001). Ubiquitination can either target substrate proteins for degradation via the 26S proteasome, change their location or alter their function (Mansour, 2018). In eukaryotic cells ubiquitination is linked to a variety of biological functions such as DNA repair, gene expression, and immunity (Komander & Rape, 2012). Since the ubiquitination process utilises multiple proteins, and is critical for maintaining homeostasis, a mutation in any one of the involved proteins could result in birth defects, cancer, or paediatric disease (Rape, 2018).

The structure of ubiquitin is comprised of a β-grasp fold, and a malleable carboxy-terminal tail comprised of six residues. The sequence of ubiquitin is quite conserved from yeast to humans suggesting that its surfaces are recognized by proteins with ubiquitin-binding domains (UBDs). (Komander & Rape, 2012). Ubiquitin can be expressed in two different forms; as a fusion to ribosomal proteins, which is encoded by genes *UBA52*, and *RPS27A* (also known as *UBA80*), or as a polyubiquitin cassette, which is encoded by genes *UBB*, and *UBC*, that is cleaved by deubiquitinases (DUBs) to generate monomers. Under duress cells have been found to increase transcription of the *UBB*, and *UBC* genes in order to swiftly increase ubiquitin levels (Rape, 2018).

The ubiquitination process culminates in the attachment of a ubiquitin polypeptide onto a lysine residue of a target protein in order to post-translationally modify it. E1 activating

enzymes, E2 conjugating enzymes, and E3 ubiquitin ligase enzymes are all involved in the adenosine triphosphate (ATP)-dependent process of ubiquitination. The mechanism of ubiquitination begins via activation of ubiquitin by an E1-activating enzyme in an ATP dependent reaction, resulting in the formation of a thioester bond between a cysteine (C) residue in the active site of E1, and the carboxy-terminal of ubiquitin. The activated ubiquitin is transferred to the E2 conjugating enzyme, once more forming a thioester bond between the carboxy-terminal of ubiquitin, and the E2 enzyme's active site (Fang & Weissman, 2004). The E3 ubiquitin ligase first recognises the substrate protein before transferring ubiquitin onto it (Buetow & Huang, 2016). Specifically, the E3 ubiquitin ligase binds the E2-ubiquitin intermediate, and the target protein in order to catalyze the formation of the isopeptide bond between the carboxy-terminal glycine (G) of ubiquitin, and the lysine residue of the substrate protein (**Figure 1.1**) (Mansour, 2018). The interaction between the E2, and E3 enzymes leads to the modification of many target proteins, as well as the specificity of ubiquitination (Hershko & Ciechanover, 1998).

The E3 ubiquitin ligase is a multisubunit complex that is responsible for substrate selection (Chan & Hill, 2001). E3 ligases are divided into three groups, each defined by the domain they possess: there is the Really Interesting New Gene (RING), Homologous to the E6AP Carboxyl (C) Terminus (HECT), and the RING-between- RING (RBR) domain. The commonality among the aforementioned domains is their ability to bind to the E2-ubiquitin, the difference among the domains is the structure, and the mechanism used for ubiquitin transfer onto a substrate protein. The largest class of E3 ligases are the RING E3 ligases as there are about 600 in humans. RING E3 ligases use their RING domain to transfer ubiquitin from the E2-ubiquitin to the substrate protein directly. Unlike RING E3 ligases, HECT E3 ligases and RBR

E3 ligases promote ubiquitin transfer to a substrate protein in a multi-step process. The catalytic cysteine in both HECT, and RBR E3 ligases obtains the ubiquitin from the E2-ubiquitin, generating an intermediate E3-ubiquitin, and then transfers the ubiquitin to the substrate protein (**Figure 1.1**) (Buetow & Huang, 2016).

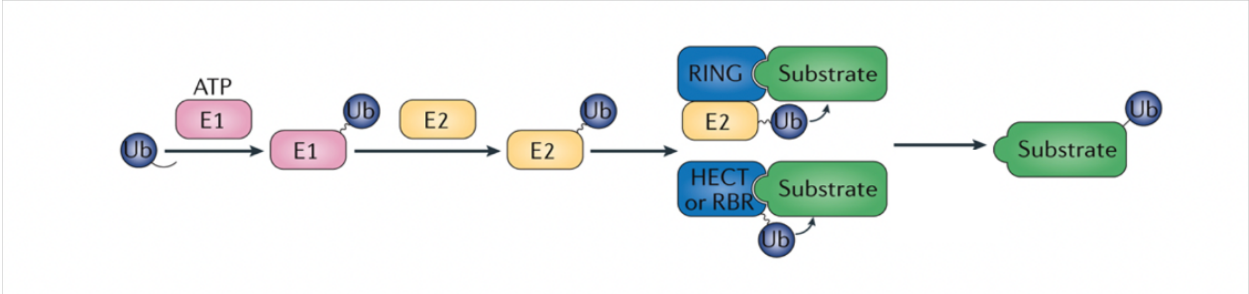

Figure 1.1. The Ubiquitination Pathway. The ubiquitination pathway begins with activation of ubiquitin by an E1-activating enzyme in an ATP dependent reaction, which is then carried by an E2 conjugating enzyme, which with the E3 ubiquitin ligase transfers the ubiquitin to the substrate protein. The E3 ubiquitin ligase then binds the E2-ubiquitin intermediate, and the substrate protein in order to form an isopeptide bond between the carboxy-terminal glycine of ubiquitin and the lysine residue of the substrate protein. There are three types of E3s: RING, HECT, and RBR. RING E3 ligases use their RING domain to transport ubiquitin from the E2-ubiquitin to the substrate protein directly. HECT E3 ligases and RBR E3 ligases obtain ubiquitin from the E2-ubiquitin forming an E3-ubiquitin intermediate, then transfer the ubiquitin to the substrate protein. Deubiquitinases can remove ubiquitin from a substrate (DUBs). Figure adapted from Rape, 2018.

There are various modifications that can be achieved via ubiquitination, which are monoubiquitination, multi-monoubiquitination or polyubiquitination. The type of modification, and the type of linkage determine the impact ubiquitination has on the target protein (Swatek & Komander, 2016). Ubiquitin contains an N-terminal methionine (M1), and seven lysine (K) residues (K6, K11, K27, K29, K33, K48 or K63) that can be further ubiquitinated leading to the formation of polyubiquitin chains (Ronau et al, 2016). Polyubiquitin chains can be homotypic in which the linkage is uniform or heterotypic in which the linkage is mixed (Akutsu et al, 2016). Heterotypic chains could become branched when one ubiquitin protein is further ubiquitinated at

two or more residues (Meyer & Rape, 2014). As a result, a variety of polyubiquitin chains can be generated, each representing a distinct intracellular signal (**Figure 1.2**) (Grice & Nathan, 2016).

Ubiquitination is well known for its role in targeting proteins for degradation by the ATP dependent 26S proteasome through the formation of polyubiquitin chains on K48 of the ubiquitin moiety (Thrower et al, 2000). Although K48 polyubiquitination is the most common linkage it is not the only signal for proteasomal degradation; K11 linked polyubiquitination, and branched heterotypic K11/K48 polyubiquitin chains, which are synthesized by the RING E3 ubiquitin ligase Anaphase Promoting Complex/Cyclosome (APC/C), were uncovered as a stronger signal for proteasomal degradation (Meyer & Rape, 2014). K63 linear polyubiquitination is a common type of ubiquitin modification that has a role in DNA repair, as K63 polyubiquitination interacts with DNA, in order to recruit repair factor such as Receptor associated protein 80 (Rap80), to direct homologous recombination (Sobhian et al, 2007; Liu et al, 2018). K63 polyubiquitination activates Transforming growth factor β Activated Kinase-1 (TAK1), which in turn activates I-kappa B Kinase complex (IKK) and Mitogen-Activated Protein (MAP) kinases ultimately leading to activation of the NF- κB pathway (Adhikari et al, 2007). Monoubiquitination was uncovered to have a role in DNA repair as Proliferating Cell Nuclear Antigen (PCNA) a DNA polymerase involved in synthesis and repair, was found to be monoubiquitinated, in order to mediate a form of DNA repair that is probably more error prone than K63 linked polyubiquitinated associated error free DNA repair (Hoege et al, 2002). Monoubiquitination was also found to be involved in endocytosis, and histone modifications **(**Dwane et al, 2017). Ubiquitinated proteins have different fates depending on which ubiquitin linkages they have (**Figure 1.2**).

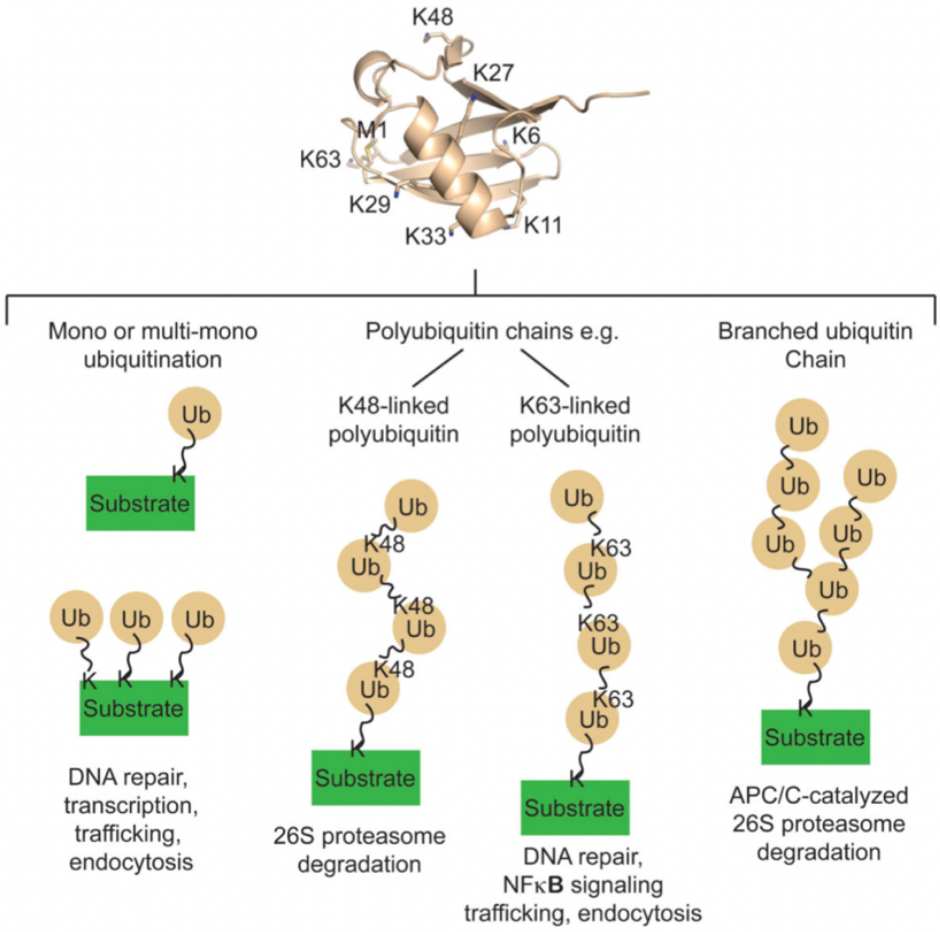

Figure 1.2. The Fate of the Ubiquitinated Protein Depends on the Type of Ubiquitin Modification. Polyubiquitination occurs when the seven lysine (K) residues of ubiquitin are further ubiquitinated, as well as the N-terminal methionine (M1). A substrate protein can be monoubiquitinated at one lysine residue or multi-mono ubiquitinated at multiple lysine residues. Lysine 48 and lysine 63 polyubiquitin linkages are homotypic, since the same residue is further ubiquitinated. When a distinct residue on a single ubiquitin polypeptide gets ubiquitinated, the result is a branched polyubiquitin chain. Different ubiquitin modifications lead to different outcomes for ubiquitinated proteins. Figure adapted from Buetow & Huang, 2016

1.2 Deubiquitination

The ubiquitin moiety on substrate proteins can be removed through the process of deubiquitination. Deubiquitination is carried out by DUBs, which are proteases that hydrolyze the ubiquitin-substrate protein isopeptide bond to remove the ubiquitin moiety (Wilkinson, 1997). As stated earlier, precursor ubiquitin can be expressed either as a fusion to ribosomal

proteins, which is encoded by genes *UBA52*, *UBA80* or as a polyubiquitin cassette, which is encoded by genes *UBB*, and *UBC*. In either case the precursor ubiquitin must be cleaved by DUBs in order to have mature ubiquitin monomers (Rape, 2018; Komander et al, 2009). In order to recycle ubiquitin in the cell, DUBs can remove the polyubiquitin chain from the substrate protein, which is then disassociated into monomers. Deubiquitination can improve protein stability since DUBs can remove polyubiquitin chains from substrate proteins before they are degraded by the 26S proteasome. Deubiquitination can also edit the ubiquitin signal via shortening the ubiquitin chain, as well as remove a non-degradative ubiquitin signal (Komander et al, 2009). Deubiquitination helps keep unanchored ubiquitin chains from competing with ubiquitinated substrates for ubiquitin binding sites in the 26S proteasome, and deubiquitination helps regulate proteolysis rates by preserving the number of ubiquitin monomers accessible in a cell (**Figure 1.3**) (Amerik & Hochstrasser, 2004).

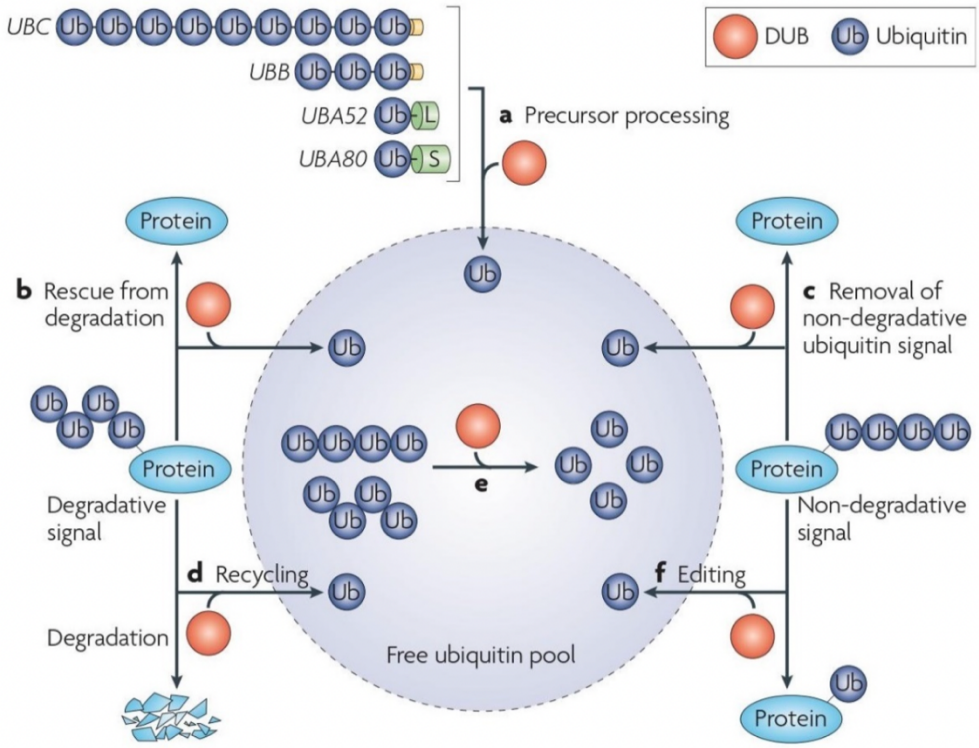

Figure 1.3. The Various Roles of DUBs in Cells. (a) Precursor ubiquitin can be expressed either a fusion to ribosomal proteins, which is encoded by genes *UBA52*, *UBA80* or as a polyubiquitin cassette, which is encoded by genes *UBB*, and *UBC*. The precursor ubiquitin must be cleaved by DUBs to generate mature ubiquitin monomers. (b) Deubiquitination can regulate protein stability since DUBs can remove polyubiquitin chains from substrate proteins before they are degraded by the 26S proteasome. (c) DUBs can remove a non-degradative ubiquitin signal (d) In order to recycle ubiquitin in the cell, DUBs remove polyubiquitin chains from the substrate protein. (e) DUBs can dismantle polyubiquitin chains into monomers. (f) Deubiquitination can also edit the ubiquitin signal via shortening the ubiquitin chain. Figure adapted from Komander et al, 2009.

There are about 100 DUBs in humans, and there are six structurally different families of DUBs (Mevissen & Komander, 2017). There are five kinds of cysteine proteases among the six families of DUBs, each of which uses a cysteine residue in the active site, as well as a neighbouring histidine (H) and aspartate (D) residue, to form a catalytic triad that allows a nucleophilic attack on the isopeptide bond between the substrate and ubiquitin (Nijman et al, 2005). The five families of cysteine proteases are ubiquitin specific proteases (USP), ubiquitin

C-terminal hydrolases (UCH), Machado-Joseph domain protease (MJD), ovarian tumour related proteases (OTU), and motif interacting with ubiquitin (MIU)-containing novel DUB family (MINDY) (Mevissen & Komander, 2017). The sixth kind of DUB is the JAB1/MPN/MOV34 metalloprotease (JAMM) family that uses a zinc (Zn) ion stabilised by an aspartate, and two histidine residues to cleave ubiquitin (Amerik & Hochstrasser, 2004).

The largest class of DUBs is USPs which are activated by binding to ubiquitin (Pfoh et al, 2015a). USPs have high sequence conservation in their catalytic domain which consists of a cysteine, histidine (H), and aspartate (D) or asparagine (N) residue, forming an active site (Komander et al, 2009). The structure of the catalytic domain of a representative USP, human Ubiquitin Specific Protease 7 (USP7) also known as Herpesvirus-Associated Ubiquitin-Specific Protease (HAUSP) was discovered to have a conserved structure consisting of a Fingers, Palm and Thumb. The Fingers coordinate the ubiquitin that is to be cleaved with its C-terminal in the active site, which is between the Palm and the Thumb (Hu et al, 2002). Substrate specificity of USPs is thought to be due to the diverse amino acid sequences of the non-catalytic domains (Pfoh et al, 2015a).

1.3 USP7

HAUSP, also known as USP7 belongs to the USP class of DUBs. USP7 is expressed in all cell types and is essential as it regulates the stability of substrate proteins involved in various cellular pathways such as epigenetics, tumour suppression, as well as DNA damage response. Therefore, aberrant USP7 expression leads to pathogenesis (Pozhidaeva and Bezsonova, 2019). USP7 is well recognized for its role in regulating p53 levels in cells, as p53 is stabilised via deubiquitination by USP7, and a reduction in USP7 levels results in decreased levels of p53 (Li et al, 2004). The E3 ubiquitin ligase Mouse double minute 2 homolog (MDM2) ubiquitinates

p53, and it was discovered that USP7 also regulates the stability of MDM2, as cells lacking USP7 had unstable self-ubiquitinated MDM2, which resulted in p53 activation (Li et al, 2004). In mice embryos that had USP7 knocked out there was a decrease in cell proliferation likely due to low levels of p53, which is known to cause cell growth arrest. The mice that lacked USP7 exhibited embryonic lethality which could not be rescued by simultaneous knockout of p53 with USP7, therefore USP7 was hypothesized to have a role outside of regulating p53 (Kon et al, 2010). Following this discovery, numerous attempts have been made to uncover the full breadth of USP7's possible roles in the cell. A recent study linked haploinsufficiency of USP7 to clinical aspects of neurodevelopmental disorders, emphasising the importance of USP7. Many of the individuals in the study had heterozygous deletions of USP7, others had nonsense, or missense mutations of USP7. These individuals exhibited intellectual disability, clinical features of autism spectrum disorder (ASD), speech delays, and seizures (Fountain et al, 2019). Overall, appropriate expression of USP7 is essential to cellular function at a molecular level, as well as normal development.

1.3.1 Structure of USP7

USP7 is an 1102 amino acid residue protein with a molecular weight of 135 kiloDaltons (kDa) that has three well defined domains. There is the tumor necrosis factor receptor-associated factor (TRAF) like domain, also referred to as Meprin and Traf Homology (MATH) domain, at the Amino-Terminal Domain (NTD), there is the central catalytic domain (CAT), and the Carboxy-Terminal Domain (CTD) that contains five ubiquitin like (Ubl 1-5) folds (**Figure 1.4**). The function of the catalytic domain of USP7, which encompasses residues 208-580, is to cleave the ubiquitin from the isopeptide bond formed with a substrate protein (Pozhidaeva and Bezsonova, 2019). As in other USPs, the fingers bind to the ubiquitin that will be cleaved, within

the CAT between the thumb, and the palm (**Figure 1.4A**) (Hu et al, 2002). The residues that form the catalytic triad of USP7 are C223, H464, and D481. The histidine residue in the CAT deprotonates cysteine's thiol group, initiating the nucleophilic attack on the isopeptide bond, and the aspartate prevents rotation of histidine's side chain which results in its polarization (Pozhidaeva and Bezsonova, 2019). USP7 is in an inactive state, which upon binding to ubiquitin causes conformational changes in the CAT and the CTD, resulting in USP7 becoming active (Faesen et al, 2011). USP7 in its active state has a more stable CAT whose ubiquitin binding conformation is stable, therefore USP7 displays improved deubiquitinase activity (Rougé et al, 2016). The catalytic domain of USP7 is essential for its deubiquitinating activity, while the N-terminal TRAF or MATH, and the C-terminal Ub1l2 domains are utilised to interact with substrate proteins (Valles et al, 2020).

The NTD of USP7 covers amino acid residues 1-208, with the TRAF, also known as MATH domain, spanning residues 63 to 208 (**Figure 1.4B**). The TRAF domain of USP7 has a similar structure to TRAF proteins, and is structured as an eight stranded, anti-parallel β sandwich (**Figure 1.4C**) (Saridakis et al, 2005). Substrate proteins that contain a (P/A/E)xxS consensus motif interact with USP7's NTD via binding to the groove on the MATH domain surface which contains a ^{164}DWGF^{167} motif in β strand 7 (**Figure 1.4C)** (Bojagora & Saridakis, 2020). Mutation of the conserved ^{164}DWGF^{167} motif of USP7, specifically the mutation of residues, aspartate (D) at position 164 (D164) and tryptophan (W) at position 165 (W165) to alanine leads to loss of interaction of USP7 with substrates p53, and MDM2. Therefore, the D and W residues of the ^{164}DWGF^{167} are essential for the interaction of substrates with the NTD of USP7 (**Figure 1.4A**) (Sheng et al, 2006). Some notable proteins that interact with the NTD of USP7 include the Epstein-Barr virus (EBV) protein, EBNA1, p53, Hdmx, Hdm2, UbE2E1, and

the Kaposi's Sarcoma Herpesvirus (KSHV) protein vIRF1 (Chavoshi et al, 2016; Saridakis et al, 2005; Sarkari et al, 2010; Sarkari et al, 2013; Sheng et al, 2006).

The CTD of USP7 spans from amino acid residues 562-1081, and contains five ubiquitin like (Ubls) folds, that are named so as their structure is similar to ubiquitin, yet their sequence is not (**Figure 1.4B**) (Faesen et al, 2011; Gagarina et al, 2019). Ubl45 is hypothesized to bind to a "switching" loop in the CAT of USP7, resulting in activation of USP7, thereby enhancing binding of ubiquitin, and increasing deubiquitinase activity by 100-fold (Faesen et al, 2011). Another study discovered that the most extreme end of USP7's CTD, which encompasses residues 1084-1102, improves deubiquitinase activity by binding the CAT's activation cleft, and stabilising USP7's active conformation (Rougé et al, 2016). A flexible hinge was discovered between Ubl2, and Ubl3, which could bring Ubl45 closer to the CAT, which would support the model that Ubl45 binds to a "switching" loop in the CAT of USP7, activating USP7, and stabilising binding of ubiquitin (Faesen et al, 2011; Pfoh et al, 2015b).

The CTD not only aids in activation of USP7, but it also contains the second interaction site of some identified USP7 substrates. Substrate proteins of USP7 that contain a conserved KxxxK or KxxxKxK motif interact with USP7 at its CTD specifically with the ^{758}DELMDGD^{764} motif in Ubl2, in which the aspartate residues, D762, and D764 of USP7 form salt bridges with the lysine residues of the substrate (**Figure 1.4D**) (Pfoh et al, 2015b). Upon mutation of the aspartate residues in the ^{758}DELMDGD^{764} motif in the Ubl12 of USP7, there is attenuated interaction with substrates, such as the Herpes Simplex Virus HSV-1 protein Infected Cell Protein 0 (ICP0), Ubiquitin-like with PHD And Ring Finger Domains 1 (UHRF1), and Enhancer of Zest Homolog 2 (EZH2) (Gagarina et al, 2019; Pfoh et al, 2015b; Zhang et al, 2015).

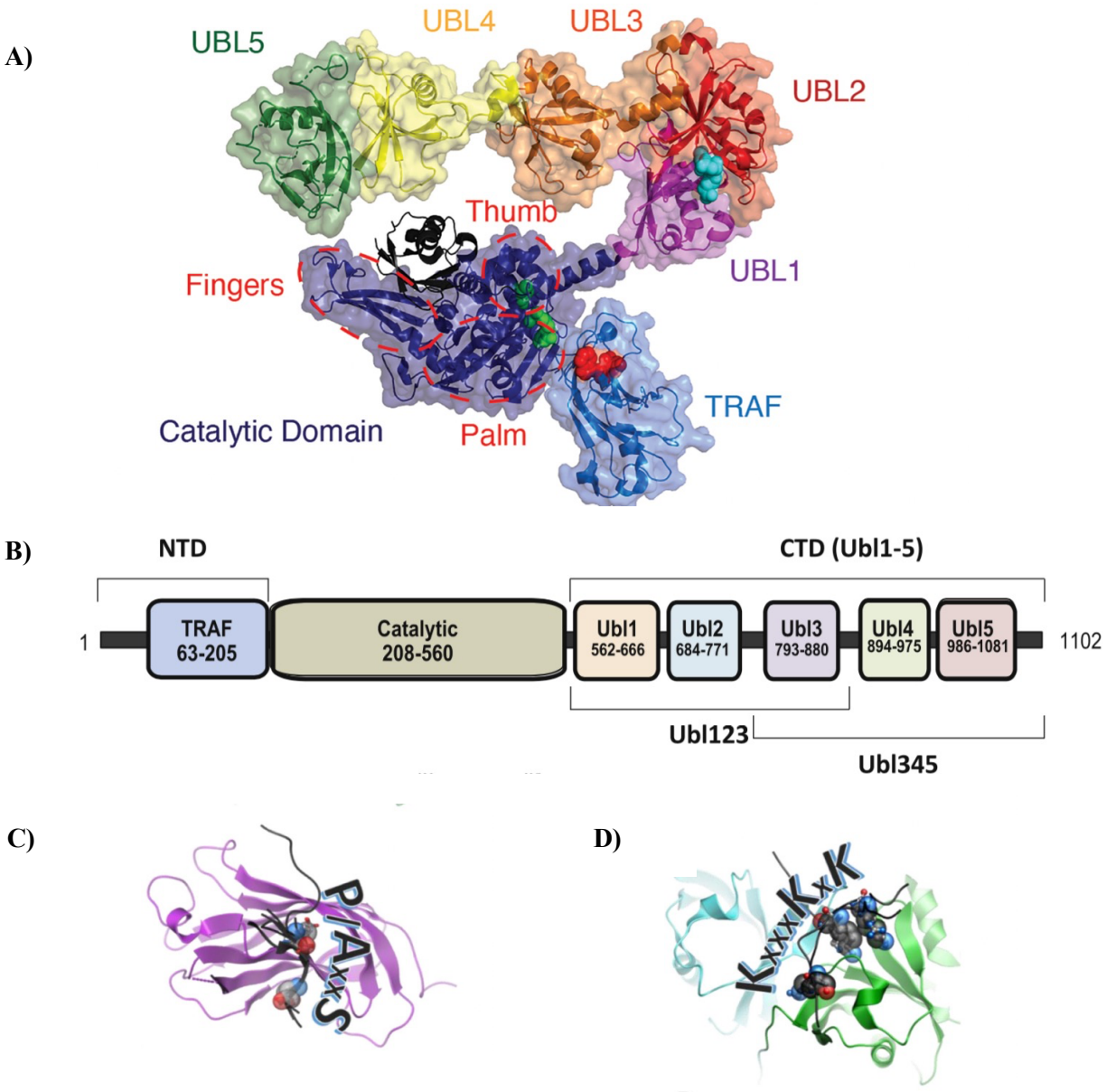

Figure 1.4. The Domain Structure of USP7 & Structure of Binding Domains. A) The D164 and W165 residues which are essential for substrates to bind to USP7's TRAF domain are shown in red spheres. The catalytic triad of USP7 comprised of residues C223, H464, and D481 are represented by green spheres. The D758, E759, and D764 residues used by Ubl2 of USP7 to interact with substrates are indicated by blue spheres. The conserved structure of USP7's catalytic domain consisting of a Fingers, Palm and Thumb is outlined by red dashes. Figure adapted from Valles et al, 2020. B) The residues comprising the N-Terminal Domain, Catalytic Domain, and C-Terminal Domain of USP7 are shown. Figure adapted from Gagarina et al, 2019. C) The TRAF/MATH domain of USP7 shown interacting with the P/AxxS motif of a peptide (black). D) the Ubl2 of the CTD of USP7 shown interacting with the KxxxKxK motif of a peptide (black). Figures C) and D) adapted from Pozhidaeva and Bezsonova, 2019.

1.3.2 USP7 is Essential for Cell Cycle Progression

The cell cycle is tightly regulated by a variety of proteins. USP7 appears to have a role in cell cycle progression as it interacts with Retinoblastoma-associated protein (Rb) a tumour suppressor protein that is well known for regulating the transition of cells from G1 to S phase of the cell cycle. Upon phosphorylation Rb is degraded by ubiquitination via MDM2, allowing the transcription factor E2F1 to activate expression of genes that allow entry into S phase. USP7 was found to interact with Rb *in vivo*, as well as *in vitro*. USP7 was discovered to deubiquitinate the K48 polyubiquitin chains of Rb, protecting Rb from proteasomal degradation, thereby resulting in its stabilisation (Bhattacharya & Ghosh, 2014).

To ensure genomic integrity, and the production of genetically identical daughter cells, genomic stability must be maintained throughout the cell cycle. The M phase kinase polo-like kinase 1 (Plk1) that is integral to mitosis, and appropriate chromatid segregation, is regulated by USP7 (Peng et al, 2019). USP7 not only deubiquitinates, and stabilises Plk1, but it also does the same for Plk1's E3 ubiquitin ligase, Checkpoint with Forkhead and Ring Finger Domains (CHFR) (Oh et al, 2007; Peng et al, 2019). Mitotic stress prevents progression into M phase by CHFR ubiquitinating Plk1, and causing its degradation (Kang et al, 2002). USP7 deficient cells are stuck in the G2/M phase of the cell cycle, and USP7 knockdown leads to an increase in cells with misaligned chromosomes during mitosis (Peng et al, 2019). USP7 deubiquitinates budding uninhibited by benzimidazoles 3 homolog (Bub3), which is involved in formation of the correct attachments between kinetochores and microtubules, as part of the Spindle Assembly Checkpoint (SAC) complex. Cells lacking USP7 display aberrant chromosomal segregation, presumed to be due to a reduction in Bub3 levels, therefore, it is assumed that USP7's stabilising effect on Bub3

levels is critical for genomic integrity (Giovinazzi et al, 2014). As a result, by stabilising CHFR, Plk1, and Bub3, USP7 is essential for genomic integrity.

USP7 has recently been discovered to play a role in cytokinesis, as it stabilises F-box only protein 38 (FBXO38), which is thought to be owing to USP7's deubiquitinase activity, since FBXO38 levels increased when USP7 was silenced in combination with the proteasome inhibitor MG-132. FBXO38 was found to stabilise kinesin family member 20B (KIF20B), an enzyme required for cytokinesis. Since silencing USP7 resulted in a decrease in KIF20B levels, and cytokinetic defects, such as the formation of multinucleated cells, it was proposed that USP7 stabilises KIF20B via stabilising FBXO38 (Georges et al, 2019). Overall, USP7 is essential for progression through the cell cycle, genomic integrity throughout mitosis, and cytokinesis.

1.3.3 Importance of USP7 in Wnt/β-catenin Signalling Pathway Activation

USP7 regulates proteins in the evolutionarily conserved Wnt/β-catenin signalling pathway, which utilises the transcription factor β-catenin to regulate the expression of cell cycle-related genes. β-catenin levels are regulated by post translational modifications; first, it is phosphorylated by Glycogen Synthase Kinase 3 (GSK3) and Casein Kinase 1 (CK1), followed by ubiquitination by the E3 ubiquitin ligase β-transducin repeats-containing proteins (β-TrCP), which leads to proteasomal degradation (**Figure 1.5**) (Nusse & Clevers, 2017). The MATH domain of USP7 is known for interacting with many substrates, including Ring Finger Protein 220 (RNF220), an E3 ubiquitin ligase. USP7 interacts with β-catenin, and this interaction was boosted by overexpression of RNF220, indicating that RNF220 is required for USP7/β-catenin interaction. The interaction between USP7 and RNF220 causes β-catenin to be deubiquitinated and stabilised, resulting in enhanced expression of Wnt target genes. In colon cancer cell lines, knocking down USP7, and RNF220 resulted in reduced levels of β-catenin, demonstrating that

USP7's interaction with RNF220 is needed for Wnt/β-catenin signalling pathway activation (Ma et al, 2014).

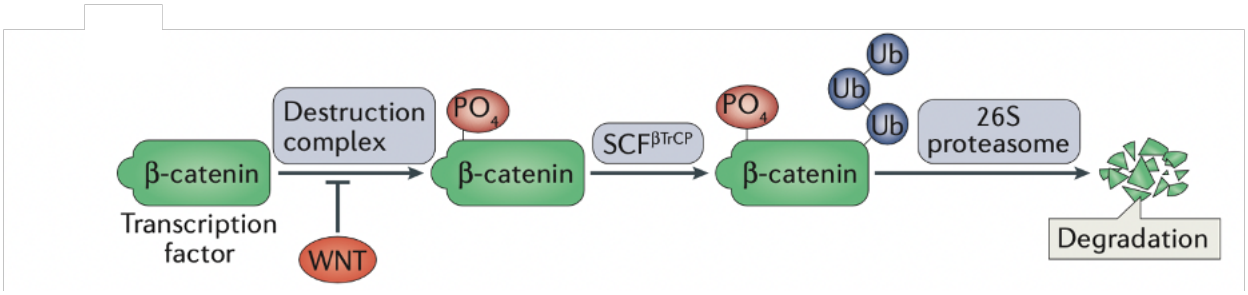

Figure 1.5. Degradation of β-catenin. β-catenin is phosphorylated, then it is ubiquitinated by β-TrCP, which leads to proteasomal degradation of β-catenin unless the Wnt/β-catenin signalling pathway is activated. Figure adapted from Rape, 2018.

A mutation in the tumour suppressor gene Adenomatous Polyposis Coli (APC) causes persistent activation of the Wnt/-catenin signalling pathway in many colorectal cancer cells (APC). APC contains a β-catenin inhibitory domain (CID) that aids in the ubiquitination of β-catenin, lowering its levels, and inhibiting the Wnt/β-catenin pathway's transcriptional activity (Nusse & Clevers, 2017). The APC gene is mutated, resulting in the creation of a shortened APC protein with no CID, which stabilises β-catenin, and keeps the Wnt/β-catenin signalling pathway active. In colorectal cancer cell lines USP7 was found to interact with β-catenin through the TRAF domain of USP7, as there were two P/A/ExxS binding sequences found within β-catenin. Truncated APC that did not contain the CID leads to stabilisation of β-catenin through deubiquitination by USP7, and continuous activation of Wnt/β-catenin signalling (Novellasdemunt et al, 2017).

It was discovered that the Zinc Finger MIZ-Type Containing 2 (ZMIZ2) protein stabilised β-catenin levels in colorectal carcinogenesis via K48 linked deubiquitination. The DUB responsible for this function was identified as USP7, and it was discovered that wild type

USP7 stabilised β-catenin protein levels, whereas the catalytically inactive mutant in which C223 was mutated to alanine (A), C223A, did not. In the nucleus ZMIZ2, β-catenin, and USP7 were discovered to interact. Similar to β-catenin the TRAF domain of USP7 was responsible for the interaction with ZMIZ2. A reduction in ZMIZ2 disrupted the interaction between USP7, and β-catenin (Zhu et al, 2020). USP7 is hypothesised to be involved in the regulation of the Wnt/β-catenin signalling pathway, which is well known for upregulating transcriptional activity of genes required for cell proliferation, by stabilising β-catenin. The substrates of USP7 involved in β-catenin regulation, as well as the interaction between USP7 and β-catenin was determined to occur via the TRAF domain at the N-terminus of USP7, which is noteworthy. Given the importance of the Wnt/β-catenin signalling pathway and USP7's various roles in cells, it is possible there are additional USP7 substrates that impact the Wnt/β-catenin signalling pathway.

1.3.4 Relevance of Targeting USP7 in Cancer Therapy

USP7 is a potential candidate as a cancer therapeutic target due to its involvement in various cellular pathways, as well as its overexpression in many cancers, such as colon, breast, and prostate cancer (Pozhidaeva and Bezsonova, 2019; Wang et al, 2019). Depending on the circumstance, and the substrate that it is interacting with, USP7's role in cancer may be as tumour suppressor or an oncogene (Bhattacharya et al, 2018). USP7 is of interest as a therapeutic target as it is involved in regulation of MDM2, and p53, which is the most frequently inactivated tumour suppressor in cancer. It has been proposed that by inhibiting USP7, MDM2 would be degraded, and p53 would be stabilised, allowing p53 to resume its role as a tumour suppressor (Bonacci & Emaneuele, 2020). A USP7 inhibitor that functions by preventing USP7 deubiquitination activity, P5091, leads to increased levels of p53, which resulted in apoptosis (Chauhan et al, 2012). As mentioned, USP7 can stabilise β-catenin in APC truncated colorectal

cancer, which can lead to constant Wnt/β-catenin signalling pathway activation (Novellasdemunt et al, 2017). P5091 was found to prevent USP7 deubiquitination of β-catenin leading to degradation of β-catenin resulting in Wnt/β-catenin pathway inactivation, therefore inhibiting colorectal tumour growth *in vivo* (**Figure 1.6**) (An et al, 2017). Though USP7 inhibitors have demonstrated success in inhibiting tumour growth, there is the potential of off-target effects as the catalytic domains of USPs are homologous. Many USP7 inhibitors have low selectivity and potency. One way to develop more selective and potent USP7 inhibitors is to find new allosteric binding sites (Li & Liu, 2020).

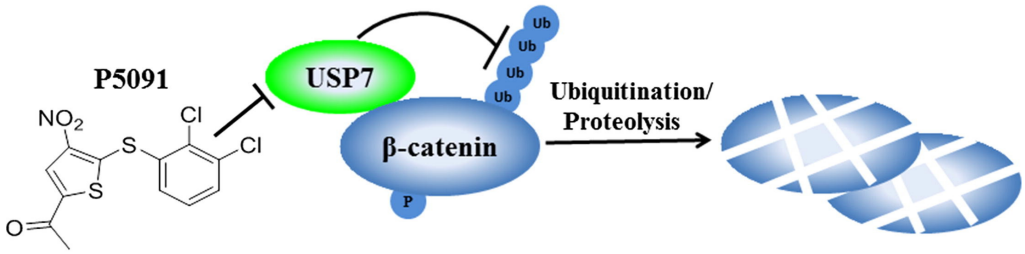

Figure 1.6. The Wnt/β-catenin Pathway is Inactivated by P5091. The USP7 inhibitor P5091 allows for the degradation of β-catenin, and inactivation of the Wnt/β-catenin pathway. Figure adapted from An et al, 2017.

1.4 FOXM1

Transcription factors are required for the regulation of gene expression in cells, which contributes to cellular homeostasis. Transcription factors' activity is tightly regulated, and they function in complexes with other transcription factors to enable gene expression. Transcription factors have Transactivation Domains (TADs) that lead to the assembly of numerous proteins required for transcription on target gene promoters. Transcription factors also have a Negative Regulatory Domain (NRD) that binds to the TAD in order to inhibit it, acting as a form of autorepression for the transcription factor (Marceau et al, 2019). Forkhead box M1 (FOXM1) is

a transcription factor of interest because it is overexpressed in cancer (Liu et al, 2021). FOXM1 belongs to the forkhead family of transcription factors as it has a conserved winged helix DNA Binding Domain (DBD), also known as the forkhead (FKH) domain (**Figure 1.7**) (Laoukili et al, 2007). The N-terminal Negative Regulatory Domain (NRD), the Cdk-site region (CSR), which contains cyclin dependent kinase consensus sites, and the C-terminal Transactivation Domain (TAD) together form the FOXM1 structure (**Figure 1.7**) (Marceau et al, 2019).

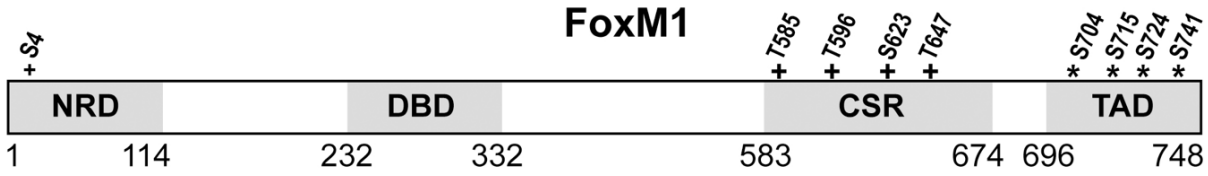

Figure 1.7. Structure of FOXM1. The Negative Regulatory Domain, DNA Binding Domain, Cdk-Site Region, and Transactivation Domain of FOXM1 are shown in grey. Figure adapted from Marceau et al, 2019.

The activity of FOXM1 is determined by its conformation. The NRD of FOXM1 reduces FOXM1 activity by interacting with its TAD; however, when FOXM1 is phosphorylated by cyclin A/cyclin dependent kinases (Cdks) during G2, the NRD no longer inhibits FOXM1 activity, resulting in FOXM1 activation (Laoukili et al, 2008). Further research revealed that Plk1 phosphorylation of serine (S) at position 715 releases the TAD of FOXM1 from its NRD, and that cyclin dependent kinase phosphorylation of the CSR enhances Plk1 recruitment to FOXM1 (**Figure 1.8**). The transcriptional coactivator CREB Binding Protein (CBP) can interact with activated FOXM1 (**Figure 1.8**) (Marceau et al, 2019). FOXM1 activation is dependent on the cell cycle stage; FOXM1 was shown to be inactive during G1/S, then activated during G2/M via phosphorylation (Laoukili et al, 2008). FOXM1's active conformation enables it to function as a transcription factor, and mediate gene expression (Laoukili et al, 2008). The DBD, also

known as the FKH domain, of FOXM1 was discovered to bind to the promoters of various cell cycle genes, including the F-Box protein S-phase kinase-associated protein 2 (Skp2), Cyclin B1, and KIF20A (Leung et al, 2001; Li et al, 2020; Wang et al, 2005). FOXM1's conformation and activity are influenced by the cell cycle.

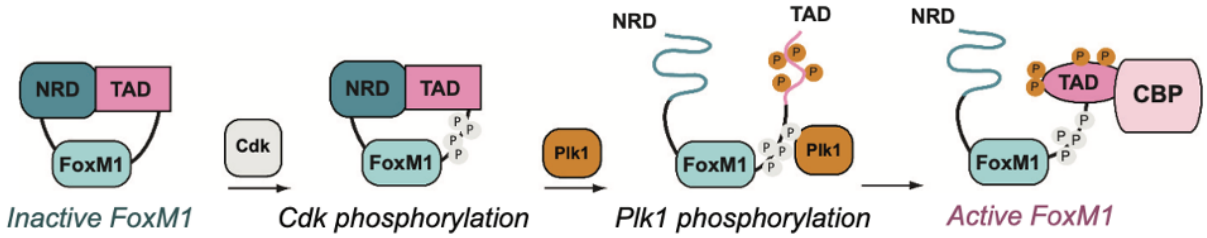

Figure 1.8. Conformational Change of FOXM1 Leads to Activation. In the early cell cycle FOXM1 is in the inactive conformation in which the NRD and TAD are interacting. Cdk phosphorylation of FOXM1 leads to Plk1 recruitment, resulting in Ser715 phosphorylation by Plk1, the TAD of FOXM1 is then released from the NRD. The active conformation of FOXM1 is able to bind to CBP in order to activate transcription. Figure adapted from Marceau et al, 2019.

1.4.1 FOXM1 is Essential to the Cell Cycle

FOXM1 expression is linked to the cell cycle since it is not expressed in differentiated cells but is found in proliferating cells (Nandi et al, 2018). FOXM1 expression begins at the beginning of the S phase, and continues through the G2, and mitotic phases of the cell cycle (Laoukili et al, 2007). FOXM1 stimulates the expression of genes involved in the cell cycle's S and M phases, including Skp2, and Cyclin B1 (Liu et al, 2021). Considering FOXM1 expression is linked to the cell cycle, it was assumed that its function as a transcription factor is as well.

The absence of FOXM1 was discovered to affect cell cycle progression, as breast cancer cells without FOXM1 lingered in the G2-M phase of the cell cycle, and cell viability was reduced. Most cells were able to enter mitosis, but were unable to complete cell division, eventually dying; however, other cells entered mitosis but did not execute cytokinesis or nuclear

division, merely exiting mitosis, generating cells with polyploid nuclei that died as well. Multiple centrosomes are found in cells transfected with short hairpin FOXM1 (shFOXM1), resulting in multiple mitotic spindles in cells undergoing mitosis, resulting in mitotic catastrophe and cell death (Wonsey & Follettie, 2005). As a result, FOXM1 is required for normal cell cycle progression as well as cell survival.

FOXM1 is required for the cell cycle, since U2OS cells lacking FOXM1 stayed in the G2 phase longer than control cells, and their chromosomes did not align or segregate properly, resulting in polyploid cells. When FOXM1 was activated, mRNA expression of genes that contribute to mitotic progression and are only expressed in G2 or mitosis, such as cyclin B, Centromere protein F (CENP-F), and Plk1 increased, but reduced in cells lacking FOXM1. The loss of mitotic entry in cells missing FOXM1 was restored when cyclin B1 was expressed, demonstrating that FOXM1 interacts with the cyclin B1 promoter to cause mitotic entry. There is less CENP-F protein on kinetochores in cells lacking FOXM1, which has been linked to chromosome misalignment, and inappropriate chromosome segregation (Laoukili et al, 2005). Cell cycle progression, and chromosomal segregation are dependent on FOXM1.

1.4.2 The Role of FOXM1 in the Wnt/β-Catenin Signalling Pathway

When the Wnt signalling pathway is activated, β-catenin is localised in the nucleus, which promotes the production of genes like c-Myc and cyclin D1, resulting in cell cycle progression. Wnt/β-catenin pathway activation causes an increase in both FOXM1, and β-catenin in the nucleus (Moon et al, 2004). The FKH domain of FOXM1 was identified to bind to β-catenin and silencing FOXM1 reduced the amount of β-catenin in the nucleus, overall β-catenin relies on its interaction with FOXM1 for nuclear localization. There was an increase in the expression of Wnt/β- catenin signalling pathway target genes like c-MYC, and cyclin D1 in

cells that overexpress FOXM1 (Zhang et al, 2011). β-catenin needs to form a complex with T-cell factor (TCF) or lymphoid enhancer factor (LEF) transcription factor 4 (TCF4), resulting in the formation of a transcription complex on promoter regions upstream of Wnt target genes called TCF binding elements (TBEs) also known as Wnt responsive elements (WREs) to activate transcription (Moon et al, 2004). FOXM1 also binds to TCF4, and in complex with β-catenin, binds to WREs to initiate Wnt target gene activation (Zhang et al, 2011). Expression of Wnt target genes then leads to progression of the cell cycle.

GSK3 phosphorylates proteins, causing them to be ubiquitinated by E3 ubiquitin ligases, and then degraded by the proteasome. Axin, a scaffolding protein, blocks β-catenin phosphorylation by GSK3, resulting in the stability of β-catenin when the Wnt/β-catenin signalling pathway is activated (Clevers & Nusse, 2012). FOXM1 interacts with Axin, which prevents GSK3 from phosphorylating FOXM1, thereby blocking polyubiquitination of FOXM1 by the E3 ligase F-Box and WD Repeat Domain Containing 7 (FBXW7), resulting in FOXM1 stability. When FOXM1 is altered so that it cannot be phosphorylated by GSK3, it is stabilised in the presence of the proteasome inhibitor MG-132, showing that FOXM1 is also stabilised by a deubiquitinase when Wnt/β-catenin is activated. Wnt treatment in combination with overexpression of USP5 resulted in a rise in FOXM1 levels, which was attributed to USP5 interacting with FOXM1, and lowering FOXM1 ubiquitination (Chen et al, 2016). Inhibitor of β-catenin and TCF4 (ICAT) is a Wnt/β-catenin antagonist that interacts with β-catenin at the same position as TCF4, as a result, β-catenin is unable to interact with TCF4 or WREs (Daniels & Weis, 2002; Graham et al, 2002). FOXM1 interacts with β-catenin at the same site as ICAT, and β-catenin binding to ICAT decreased as FOXM1 expression. ICAT is blocked from interacting with β-catenin when FOXM1 binds to it resulting in enhanced recruitment of β-catenin to

WREs, and increased expression of Wnt target genes like c-MYC (Chen et al, 2016). As a result, FOXM1 is involved in the Wnt/β-catenin signalling pathway.

1.4.3 FOXM1 Stability is Regulated by The Ubiquitin Proteasome System

The ubiquitin proteasome system (UPS) has been implicated in the regulation of FOXM1, which in turn regulates the cell cycle. Ubiquitination of FOXM1 by the APC/C and its adaptor Cdh1, leads to FOXM1 degradation at the end of mitosis (Park et al, 2008). After Wnt/β-catenin activation, a mutant FOXM1 that could not be phosphorylated by GSK3, was stabilised in the presence of proteasome inhibitor MG-132, suggesting that a deubiquitinase stabilises FOXM1 (Chen et al, 2016). Many DUBs have been linked to the regulation of FOXM1 stability.

Ubiquitin specific protease 5 (USP5), which contributes to protein degradation through disassembly of polyubiquitin chains, expression correlates with FOXM1 (Nakajima et al, 2014). The knockdown of USP5 inhibited the proliferation of pancreatic ductal adenocarcinoma (PDA) cells, which was thought to be due to a decrease in FOXM1 protein levels, was rescued by inhibiting the proteasome with MG-132 treatment, indicating that FOXM1 is regulated by proteasome-mediated degradation. FOXM1 was discovered to be a substrate of USP5, and overexpression of USP5 prevented FOXM1 degradation, extending its half-life (Li et al, 2017). Wnt treatment in combination with overexpression of USP5 resulted in a rise in FOXM1 levels, which was attributed to USP5 interacting with FOXM1, and lowering FOXM1 ubiquitination. Wnt induced cell proliferation was decreased when USP5 was knocked out, but this effect was reversed when FOXM1 was overexpressed at the same time. The Wnt/β-catenin signalling pathway regulates the expression of FOXM1, and cyclin D1, and USP5 protein levels correlates to their levels (Chen et al, 2016). The amount of USP5, which regulates FOXM1, has an effect on cell proliferation.

Another DUB involved in FOXM1 regulation is ubiquitin specific protease 22 (USP22), which is known to deubiquitinate histones H2A, and H2B, allowing transcription of genes essential in cell cycle progression to be activated, while USP22 depletion induces cell cycle arrest in the G1 phase (Zhang et al, 2008). Further research revealed that USP22 promotes cell cycle progression by upregulating FOXM1. Overexpression of USP22 boosted proliferation by facilitating the transition of PDA cell lines from G1 to S phase, but when FOXM1 was simultaneously reduced via siRNA, this effect was no longer observed. Overexpression of USP22 resulted in increased FOXM1 and β-catenin in the nucleus, while siRNA mediated knockdown had an opposing effect. There was no change in FOXM1 nuclear localization after knocking down β-catenin via siRNA and overexpressing USP22, indicating that USP22's impact on FOXM1 is dependent on β-catenin's nuclear localization (Ning et al, 2014). As a result, USP22 influences FOXM1 levels, which in turn impacts the cell cycle.

USP28 is a DUB linked to cell cycle progression and FOXM1 stability. Overexpression of USP28 resulted in a decrease of cells in the G1 phase, followed by an increase of cells in the S phase, whereas USP28 knockdown resulted in cell cycle arrest in the G1 phase. There is a larger level of nuclear β- catenin in prostate cancer cells with elevated USP28. Wnt/β-catenin target genes c-MYC, cyclin-D1, and vascular endothelial growth factor (VEGF) all increased in response to increased USP28 expression. An inhibitor of the Wnt/β-catenin signalling pathway, XAV-939, suppressed the increase in cell proliferation caused by overexpression of USP28. Similar to nuclear β-catenin, when USP28 is overexpressed, FOXM1 levels rise. FOXM1 inhibition and silencing diminish nuclear β-catenin, even when USP28 is overexpressed, implying that FOXM1 is implicated in USP28's stimulation of the Wnt/β-catenin signalling pathway. USP28 and FOXM1 interact, and MG-132 treatment reverses the reduction in FOXM1

caused by USP28 silencing. USP28 stimulates cell proliferation in pancreatic cancer via stabilising FOXM1, which leads to nuclear β-catenin stabilisation (Chen et al, 2021).

Various DUBs have been discovered to modulate the amount of FOXM1 in mammalian cells, hence regulating cell cycle progression. Following stimulation of the Wnt/β-catenin signalling pathway, the aforementioned DUBs interact with FOXM1 to deubiquitinate FOXM1, stabilising its levels. As a result, nuclear FOXM1 accumulates and interacts with β-catenin, preventing ICAT from binding to β-catenin. Wnt target gene promoters are bound by FOXM1 complexed with β-catenin and TCF4, enhancing the expression of genes essential for cell proliferation (Chen et al, 2016).

1.4.4 FOXM1 is Implicated in Tumorigenesis

The cell cycle is highly regulated, and faulty cell cycle regulation can result in mitotic catastrophe ending in cell death or tumorigenesis. FOXM1 has been extensively researched for its role in cell proliferation and is considered an oncogene as its high expression contributes to tumour progression (Kalathil et al, 2021). Since it was discovered that FOXM1 stability affects the expression of genes required for cell cycle progression, there has been a greater focus on how FOXM1 stability is regulated. The tumour suppressor p53 was found to negatively regulate FOXM1 since FOXM1 levels increased upon mutation or inactivation of p53 (Pandit et al, 2009). As mentioned FOXM1 degradation occurs via ubiquitination through the APC/C, and FOXM1 stabilisation occurs via deubiquitination by various USPs (Chen et al, 2016; Chen et al, 2021; Li et al, 2017; Ning et al, 2014; Park et al, 2008; Zhang et al, 2011). FOXM1 over expression is associated with various cancers, such as breast cancer, ovarian cancer, and prostate cancer (Koo et al, 2012). Various studies have shown that downregulating FOXM1 levels by RNA interference results in lower cell proliferation (Ning et al, 2014; Wang et al, 2005).

Increased stability of FOXM1 via deubiquitination has been associated with tumour progression, and poor prognosis in ovarian cancer (Wang et al, 2016). Although no FOXM1 inhibitors are currently in clinical trials, it is possible to target FOXM1 by disrupting its interactions with other proteins or by promoting its degradation via the proteasome (Liu et al, 2021).

1.5 Thesis Rationale

The contents of this thesis explore the relationship between USP7 and FOXM1. FOXM1 is hypothesized to be a substrate of USP7 as it contains many conserved (P/A/E)xxS sequences. One of the conserved sequences FOXM1 contains is the PSTS binding motif of known USP7 substrate MDM2 (Sheng et al, 2006). FOXM1 also contains an EGPS motif that is known to facilitate interaction between USP7 and the viral proteins, vIRF1, and EBNA1 (Chavoshi et al, 2016; Saridakis et al, 2005). Therefore, FOXM1 is predicted to interact with the ^{164}DWGF^{167} motif in the TRAF domain at the NTD of USP7 (**Figure 1.9**). FOXM1 was hypothesized to interact with USP7 *in vitro*, and in mammalian cell lines *in vivo*. Various pull-down experiments were used to characterize the interaction between USP7, and FOXM1. As USP7 is best known for removing the ubiquitin moiety from substrate proteins, thereby preventing degradation via the 26S proteasome, the stability of FOXM1 is hypothesized to be impacted by the level of USP7 in mammalian cell lines. The regulatory role USP7 may play in FOXM1 stability was explored through various *in vivo* assays. Previous studies demonstrated that FOXM1 stability is dependent on ubiquitin-mediated proteasomal degradation, therefore USP7 may interact with FOXM1, and regulate its stability.

MKTSPRRPLILKRRRLPLPVQNAPSETSEEEPKRSPAQQESNQAEASKEVAESNSCKFPA
GIKIINHPTMPNTQVVAIPNNANIHSIITALTAKGKESGSSGPNKFILISCGGAPTQPPGLRP
QTQTSYDAKRTEVTLETLGPKPAARDVNLPRPPGALCEQKRETCADGEAAGCTINNSLS
NIQWLRKMSSDGLGSRSIKQEMEEKENCHLEQRQVKVEEPSRPSASWQNSVSERPPYSY
MAMIQFAINSTERKRMTLKDIYTWIEDHFPYFKHIAKPGWKNSIRHNLSLHDMFVRETS
ANGKVSFWTIHPSANRYLTLDQVFKQQKRPNPELRRNMTIKTELPLGARRKMKPLLPRV
SSYLVPIQFPVNQSLVLQPSVKVPLPLAASLMSSELARHSKRVRIAPKVLLAEEGIAPLSS
AGPGKEEKLLFGEGFSPLLPVQTIKEEEIQPGEEMPHLARPIKVESPPLEEWPSPAPSFKEE
SSHSWEDSSQSPTPRPKKSYSGLRSPTRCVSEMLVIQHRERRERSRSRRKQHLLPPCVDE
PELLFSEGPSTSRWAAELPFPADSSDPASQLSYSQEVGGPFKTPIKETLPISSTPSKSVLPRT
PESWRLTPPAKVGGLDFSPVQTPQGASDPLPDPLGLMDLSTTPLQSAPPLESPQRLLSSEP
LDLISVPFGNSSPSDIDVPKPGSPEPQVSGLAANRSLTEGLVLDTMNDSLSKILLDISFPGL
DEDPLGPDNINWSQFIPELQ

Figure 1.9. FOXM1 Amino Acid Sequence. FOXM1 amino acid sequence, with the (P/A/E)xxS motifs that may enable interaction with the ^{164}DWGF^{167} motif in the TRAF domain at the NTD of USP7 underlined.

CHAPTER 2: MATERIALS AND METHODS

2.1 Plasmids

The plasmids used for bacterial transformation, and expression were His-USP7 NTD, and His-USP7^{DW} NTD. The plasmids used for mammalian transfection were pCS2/FLAG-FOXM1, pcDNA3/MYC, pcDNA3.1/FLAG, pCAN/Myc-USP7, and pCAN/Myc-USP7$^{DW\text{-}MRGR}$.

2.2 Nickel Affinity Chromatography

Bacterial pellets expressing 6x-His-USP7-NTD and 6x-His-USP7^{DW}-NTD were resuspended in Binding/Lysis Buffer (50mM Tris pH 7.5, 500 mM NaCl, 5 mM Imidazole), supplemented with 1X protease inhibitor cocktail (Roche cOmplete™ Protease Inhibitor Cocktail, 11836145001), 1 mM Benzamide Hydrochloride, and 1 mM Phenylmethylsulfonyl fluoride (PMSF). The bacterial cells were lysed via sonication at 10% amplitude for 10 seconds (1 second ON, 10 seconds OFF). The lysates were clarified via centrifugation at 17,000 x g, for 10 minutes at 4°C. 1 mL of Nickel beads were equilibrated through three washes with 5 mL of Binding/Lysis Buffer. The lysates were incubated with 1mL of Nickel beads for 1 hour at 4°C on a nutator, the volume was brought to 5 mL with Binding/Lysis Buffer. The beads were then washed with Nickel Wash Buffer (500 mM NaCl, 20 mM Imidazole, 5% Glycerol). The respective beads were stored at -80°C in 500 µL 1X TBS (50 mM Tris pH 8.0, 150 mM NaCl).

2.3 His Pull-Down Assay

U2OS cells (15 cm tissue culture dish) were transfected with 10 µg of FLAG-FOXM1 using 30 µL of PolyJet™ In Vitro DNA Transfection Reagent (Signagen SL100688). After 24 hours the cells were harvested, and resuspended in 800 µL of Nonidet P-40 (NP-40) buffer (50 mM Tris- HCl pH 7.5, 150 mM NaCl, 1.0% Nonidet P-40) along with 1X protease inhibitor

cocktail (Roche cOmplete™ Protease Inhibitor Cocktail, 11836145001), 1 mM Benzamide Hydrochloride, and 1 mM PMSF, followed by gentle agitation at 4°C for 30 minutes. The cell lysate was cleared using centrifugation at 17,000 x g, for 15 minutes at 4°C. The lysate was quantified through a BCA assay using the Pierce BCA Protein Assay Kit (Thermo Scientific, 23225). For the His-pulldown, 50 µL of each 6xHis-USP7-NTD, and 6xHis-USP7^{DW}-NTD, as well as empty nickel beads were washed with 500 µL of NP-40 buffer three times. The equilibrated beads were combined with 500 µg of the lysate for 2 hours on a nutator at 4°C, the volume of the reaction was brought to 500 µL with NP-40 buffer, and 1X protease inhibitor cocktail (Roche cOmplete™ Protease Inhibitor Cocktail, 11836145001), 1 mM Benzamide Hydrochloride, and 1 mM PMSF. The beads were then washed three times with 1 mL of high salt wash buffer (50 Tris pH 8.0, 500 mM NaCl, 20 mM Imidazole, 0.1% NP-40) in 5-minute intervals on a nutator at 4°C. 50 µL of His Elution Buffer (500 mM NaCl, 500 mM Imidazole) was added to the beads, and incubated for 5 minutes. After the incubation the elution sample was prepared with 1X SDS. The inputs (5%), and elution (30 µL) were ran on a 12% SDS-PAGE gel, transferred at 90V for 2.5 hours on ice to a PVDF membrane, then blotted with 1:1,000 mouse anti-His (Santa Cruz SC-8036), and 1:2,000 mouse anti-FLAG (Sigma Aldrich F1804).

2.4 Mammalian Cell Culture, Transfection, and Sample Preparation

Human osteosarcoma U2OS cells, colorectal carcinoma cell line HCT116 parental, and HCT116 USP7$^{-/-}$ cells were grown on McCoy's (Wisent) media containing 10% fetal bovine serum (FBS), and 1 mg/ml Penicillin- Streptomycin. Human cervical adenocarcinoma cell line HeLa was grown on Dulbecco's Modified Eagle Medium (DMEM, Wisent) media containing 10% FBS, and 1 mg/ml Penicillin- Streptomycin. The cell lines were incubated at 37°C, 5%

CO_2. The cells were transfected using PolyJet™ In Vitro DNA Transfection Reagent (SignaGen Laboratories, SL100688) according to the manufacturer's protocol. Cell pellets were resuspended in Nonidet P-40 (NP-40) buffer (50 mM Tris- HCl pH 7.5, 150 mM NaCl, 1.0% Nonidet P-40) supplemented with 1X protease inhibitor cocktail (Roche cOmplete™ Protease Inhibitor Cocktail, 11836145001), 1 mM Benzamide Hydrochloride, and 1 mM PMSF, followed by gentle agitation at 4°C for 30 minutes. Cell lysates are then cleared using centrifugation for 10 minutes at 17,000 x g, 4°C. The concentration of the cell lysates were determined via a BCA assay using the Pierce BCA Protein Assay Kit (Thermo Scientific, 23225). The samples were prepared by boiling the lysates with 1X SDS.

2.5 Antibodies and Immunoblotting

The antibodies used for immunoprecipitation, and immunoblotting include rabbit anti-USP7 (Bethyl, A300-033A), mouse anti-USP7 (Millipore, 05-1946), mouse anti-MYC (Invitrogen, R950-25), mouse anti-MYC (Millipore, 05-724), rabbit anti-FOXM1 (Cell Signaling Technology, 20459), mouse anti-FLAG (Sigma Aldrich F1804), mouse anti-GAPDH (Santa Cruz SC-047723), and rabbit anti-IgG antibody (Cell Signaling, 2729). Secondary HRP-conjugated anti-mouse IgG (Jackson ImmunoResearch, 115-035-166), and anti-rabbit IgG (Cell Signaling Technology, 7074S) were used, as well as rabbit trueblot anti-rabbit IgG HRP (Rockland, 18-8816-33). All antibodies were used according to manufacturer instructions.

2.6 Proteasomal Inhibition Using MG-132

HCT116 parental, and HCT116 $USP7^{-/-}$ cells were incubated with DMSO or 20 μM of MG-132 for 2 hours. Whole cell lysates (40 μg) were resolved on a 10% SDS-PAGE gel and

transferred to a PVDF membrane at 90V on ice for 2.5 hours, then blotted with 1:20,000 mouse anti-GAPDH, 1:2,000 rabbit anti-FOXM1, and 1:1,000 mouse anti-USP7.

2.7 MYC-USP7 and FLAG-FOXM1 Co-immunoprecipitation

To test for interaction between MYC-USP7, and FLAG-FOXM1, U2OS cells were transfected with 5 μg each of both MYC-USP7, and FLAG-FOXM1 using 15 μL of PolyJet™. U2OS cells were lysed in Nonidet P-40 (NP-40) buffer (50 mM Tris- HCl pH 7.5, 150 mM NaCl, 1.0% Nonidet P-40) along with 1X protease inhibitor cocktail (Roche cOmplete™ Protease Inhibitor Cocktail, 11836145001), 1 mM Benzamide Hydrochloride, and 1 mM PMSF, followed by gentle agitation at 4°C for 30 minutes. Cell lysates are then cleared using centrifugation at 17, 000 x g, for 10 minutes at 4°C. The concentration of the cell lysates were determined via a BCA assay using the Pierce BCA Protein Assay Kit (Thermo Scientific, 23225). Cell lysates were immunoprecipitated with anti-USP7 antibody, anti-FOXM1 antibody, with rabbit IgG as a negative control. Samples were incubated overnight on a nutator at 4°C, followed by incubation with precleared Protein A/G agarose beads (Santa Cruz, sc-2003) for two hours. Immunoprecipitants were washed with 500 μL of NP-40 buffer, and boiled in 1X SDS sample buffer for 5 minutes at 100°C. The inputs (5%), and elutions (25 μL) were resolved on a 12% SDS-PAGE gel, transferred at 90V for 2.5 hours, then immunoblotted with 1:5,000 mouse anti-MYC (Invitrogen, R950-25), and 1:2,000 mouse anti-FLAG antibodies.

2.8 Endogenous Co-immunoprecipitation of USP7 and FOXM1

To test for endogenous co-immunoprecipitation between USP7, and FOXM1, HeLa cells were lysed in 800 μL of NETN Buffer (100 mM NaCl, 20 mM Tris pH 8.0, 0.5 mM EDTA pH 8.0, 0.5% NP-40), supplemented with 1X protease inhibitor cocktail (Roche cOmplete™

Protease Inhibitor Cocktail, 11836145001), 1 mM Benzamide Hydrochloride, and 1 mM PMSF, followed by gentle agitation at 4°C for 30 minutes. Cell lysates are then cleared using centrifugation at 17,000 x g, for 15 minutes at 4°C. The concentration of the cell lysates were determined via a BCA assay using the Pierce BCA Protein Assay Kit (Thermo Scientific, 23225). The lysate was precleared by incubation with 20 µL of Protein A/G-PLUS Agarose (Santa Cruz, sc-2003), and 1 µg of normal rabbit IgG at 4°C for 30 min. The beads were pelleted by centrifugation at 1,000 x g for 5 min at 4°C, and the precleared lysate was collected. To set up the endogenous immunoprecipitation reaction, 1 mg of the precleared lysate was incubated with 2 µg of rabbit anti-USP7 antibody, supplemented with NETN buffer, 1X protease inhibitor cocktail (Roche cOmplete™ Protease Inhibitor Cocktail, 11836145001), 1 mM Benzamide Hydrochloride, and 1 mM PMSF, to bring the final volume of the reaction to 500 µL. The reaction was incubated overnight at 4°C on a nutator. The following day 50 µL of Protein A/G-PLUS Agarose beads were washed thrice with 500 µL of PBS, then blocked with 5% BSA in PBS for 30 minutes at 4°C on a nutator. The beads were then equilibrated through washing with 500 µL of NETN buffer three times. The overnight antibody, and lysate reaction was added to the equilibrated beads, and incubated for 1 hour at 4°C on a nutator. The beads were washed with 500 µL of NETN buffer three times. To prepare the elution samples, 35 µL of 5X SDS was added to the beads, and boiled for 5 minutes. The input (5%), and elution (25 µL) were resolved on a 10% SDS-PAGE gel and transferred to a PVDF membrane overnight at 4°C, then blotted with 1:1,000 mouse anti-USP7, and 1:1,000 rabbit anti-FOXM1.

2.9 FLAG-FOXM1 and MYC-USP7 Interaction Site Mutant Co-immunoprecipitation

U2OS cells (15 cm tissue culture dish) were co-transfected with 5 μg of pcDNA3.1/FLAG, and MYC-USP7, as well as 5 μg of FLAG-FOXM1 with 5 μg of either MYC-USP7, or MYC-USP7$^{DW\text{-}MRGR}$, using 30 μL of PolyJet™. The cells were harvested 48 hours after transfection, and lysed in M2 Lysis Buffer (50mM Tris pH 8.0, 150 mM NaCl, 1mM EDTA pH 8.0, 1% Triton X-100), supplemented with 1X protease inhibitor cocktail (Roche cOmplete™ Protease Inhibitor Cocktail, 11836145001), 1 mM Benzamide Hydrochloride, and 1 mM PMSF, using gentle agitation at 4°C for 30 minutes. Cell lysates are then cleared using centrifugation at 17,000 x g, 15 minutes at 4°C. The supernatant was quantified using the Pierce BCA Protein Assay Kit (Thermo Scientific, 23225). Anti-FLAG M2 Affinity Gel (Sigma Aldrich A2220) was equilibrated according to the manufacturer's directions. The immunoprecipitation reactions were set up using 1 mg of clarified lysate with 40 μL of equilibrated Anti-FLAG M2 Affinity Gel, the reaction volume was brought to 1 mL using M2 Lysis Buffer supplemented with 1X protease inhibitor cocktail (Roche cOmplete™ Protease Inhibitor Cocktail, 11836145001), 1 mM Benzamide Hydrochloride, and 1 mM PMSF. The immunoprecipitation reactions were incubated overnight at 4°C on a nutator. The next day the reactions were washed four times with 500 μL of 1X TBS (50 mM Tris pH 8.0, 150 mM NaCl). The beads were boiled with 10 μL of 5X SDS. The inputs (5%), and elution (10 μL) were resolved on a 7.5% SDS-PAGE gel, and transferred to a PVDF membrane at 90V on ice for 2.5 hours. The membrane was blotted with 1:2,000 mouse anti-FLAG (Sigma Aldrich F1804), and 1:1,000 mouse anti-MYC (Millipore, 05-724).

2.10 Ectopic USP7 Expression in HeLa Cells

To understand the impact USP7 has on endogenous levels of FOXM1, HeLa cells (10 cm tissue culture dish) were transfected with 5 μg of either empty vector pcDNA3/MYC, wild type MYC-USP7, or the catalytically inactive MYC-USP7^{C223S} using 15 μL of PolyJet™. After 48 hours the cells were collected, and lysed in lysed in NP-40 buffer, supplemented with 1X protease inhibitor cocktail (Roche cOmplete™ Protease Inhibitor Cocktail, 11836145001), 1 mM Benzamide Hydrochloride, and 1 mM PMSF, using gentle agitation at 4°C for 30 minutes. Cell lysates are then cleared using centrifugation at 17,000 x g, for 10 minutes at 4°C. The cell lysates' concentrations were determined via a BCA assay using the Pierce BCA Protein Assay Kit (Thermo Scientific, 23225). The cell lysates were boiled with 1X SDS, and 40 μg of each cell lysate was resolved on a 10% SDS-PAGE gel, then transferred to a PVDF membrane at 90V for 2.5 hours on ice, then blotted with 1:10,000 mouse anti-GAPDH, 1:2,000 rabbit anti-FOXM1, and 1:1,000 mouse anti-MYC (Millipore, 05-724).

2.11 USP7 Reconstitution in HCT116 USP7$^{-/-}$ Cells

HCT116 USP7$^{-/-}$ cells were transfected with 5 μg of empty vector pcDNA3/MYC or MYC-USP7, using 10 μL of PolyJet™. The cells were harvested 24 hours later, and lysed in NP-40 buffer, supplemented with 1X protease inhibitor cocktail (Roche cOmplete™ Protease Inhibitor Cocktail, 11836145001), 1 mM Benzamide Hydrochloride, and 1 mM PMSF, using gentle agitation at 4°C for 30 minutes. Cell lysates are then cleared using centrifugation at 17,000 x g, for 10 minutes at 4°C. The cell lysates' concentrations were determined via a BCA assay using the Pierce BCA Protein Assay Kit (Thermo Scientific, 23225). The cell lysates were boiled with 1X SDS and 20 μg of each cell lysate was resolved on a 10% SDS-PAGE gel, then

transferred to a PVDF membrane at 90V for 2.5 hours on ice, then blotted with 1:10,000 mouse anti-GAPDH, 1:2,000 rabbit anti-FOXM1, and 1:1,000 mouse anti-MYC (Millipore, 05-724).

2.12 USP7 siRNA Knockdown Assay

USP7 knockdown was done using siUSP7, and siNC (negative control) (Shanghai GenePharma), the double stranded siRNA sequences used are shown in **Table 2-1**. To transfect the siRNA Lipofectamine3000™ Reagent was used according to the manufacturer's instructions. In order to see the impact on FOXM1, an siRNA mediated knockdown of USP7 was done in HeLa cells. 434 pmol of siNC or siUSP7 was transfected into 10 cm plates of HeLa cells using 43 μL of Lipofectamine3000™ Reagent. The cells were harvested 96 hours later, and lysed in NP-40 buffer, supplemented with 1X protease inhibitor cocktail (Roche cOmplete™ Protease Inhibitor Cocktail, 11836145001), 1 mM Benzamide Hydrochloride, and 1 mM PMSF, using gentle agitation at 4°C for 30 minutes. Cell lysates are then cleared using centrifugation at 17,000 x g, for 10 minutes at 4°C. The cell lysates' concentrations were determined via a BCA assay using the Pierce BCA Protein Assay Kit (Thermo Scientific, 23225). The cell lysates were boiled with 1X SDS, and 40 μg of each cell lysate was resolved on a 10% SDS-PAGE gel, then transferred to a PVDF membrane at 90V for 2.5 hours on ice, then blotted with 1:20,000 mouse anti-GAPDH, 1:2,000 rabbit anti-FOXM1, and 1:1,000 mouse anti-USP7.

Table 2.1. The Double Stranded Sequences used for siRNA Knockdowns. The siRNA sequences were transiently transfected into HeLa cells using Lipofectamine3000™ Reagent. The siNC was the negative control used, and siUSP7 was used to knockdown USP7.

siRNA	**Double Stranded Sequence**
siUSP7	5'CCCAAAUUAUUCCGCGGCAAATT3' 5'UUUGCCGCGGAAUAAUUUGGGTT3'
siNC	5'UUC UCC GAA CGU GUC ACG UTT3' 5'ACG UGA CAC GUU CGG AGA ATT3'

CHAPTER 3: RESULTS

3.1. FOXM1 Stability is Dependent on Ubiquitin Proteasome System

In order to determine if FOXM1's stability is dependent on the ubiquitin proteasome system, the cell lysates of HCT116 parental, and HCT116 USP7$^{-/-}$ cells were treated with either 20 μM of the proteasome inhibitor MG132 or the control, DMSO for 2 hours (**Figure 3.1**). In both cell lines treated with MG-132 FOXM1 was stabilised compared to the DMSO control (**Figure 3.1**).

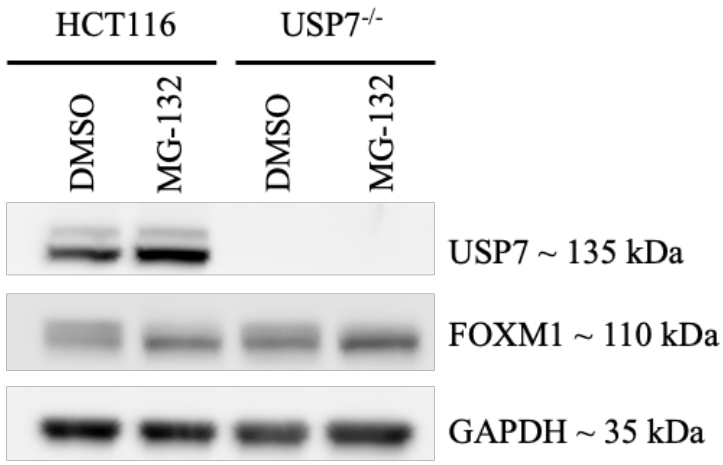

Figure 3.1. FOXM1 Stability Depends on Ubiquitin Proteasome System. HCT116 parental, and HCT116 USP7$^{-/-}$ cells were treated with 20 μM of MG132 or the control, DMSO for 2 hours before harvesting. Cellular lysates (40 μg) were resolved on a 10% gel, then blotted with mouse anti-USP7, rabbit anti-FOXM1, and mouse anti-GAPDH antibodies. n = 2.

3.2 FOXM1 and USP7 Interact *In Vivo*

To investigate the interaction between FOXM1 and USP7 *in vivo* various pull-down assays were conducted. The pull-down assays included an immunoprecipitation in HeLa cells using endogenously expressed proteins, and an immunoprecipitation in U2OS cells using ectopically expressed fusion proteins including wild type and interaction site mutants of MYC-USP7.

3.2.1 Endogenous Interaction Between USP7 and FOXM1 *In Vivo*

In order to test for endogenous interaction between USP7 and FOXM1, a co-immunoprecipitation assay was done using HeLa whole cell lysates (**Figure 3.2**). Rabbit IgG was used as a negative control. FOXM1 co-immunoprecipitated strongly with USP7 when immunoprecipitated with rabbit anti-USP7, and FOXM1 bound to rabbit IgG to some extent (**Figure 3.2**).

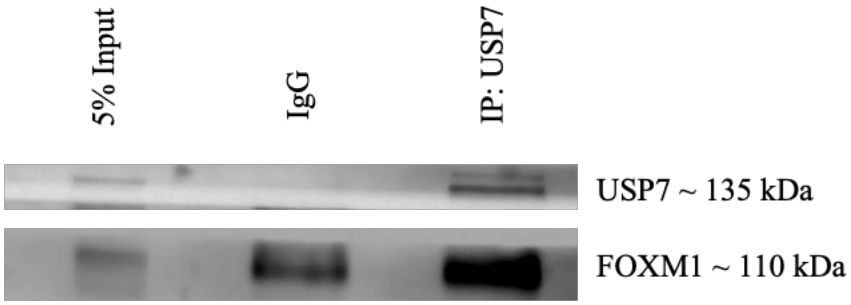

Figure 3.2. Endogenous USP7 and FOXM1 Interact *In Vivo*. U2OS whole cell lysates were immunoprecipitated with rabbit anti-USP7, using rabbit IgG as a negative control, followed by binding to Protein A/G beads. Immunoblotting was done using mouse anti-USP7 and rabbit anti-FOXM1 antibodies.

3.2.2 MYC-USP7 and FLAG-FOXM1 Interact *In Vivo*

To test whether MYC-USP7 interacts with FLAG-FOXM1, a co-immunoprecipitation was done with U2OS cells overexpressing both MYC-USP7, and FLAG-FOXM1 (**Figure 3.3**). Rabbit IgG was used as a negative control. FLAG-FOXM1 co-immunoprecipitated with MYC-USP7 when immunoprecipitated with rabbit anti-USP7, but not with rabbit IgG (**Figure 3.3A**). A reciprocal immunoprecipitation was done with rabbit anti-FOXM1, in which MYC-USP7 co-immunoprecipitated with FLAG-FOXM1, whereas it did not interact with rabbit IgG (**Figure 3.3B**).

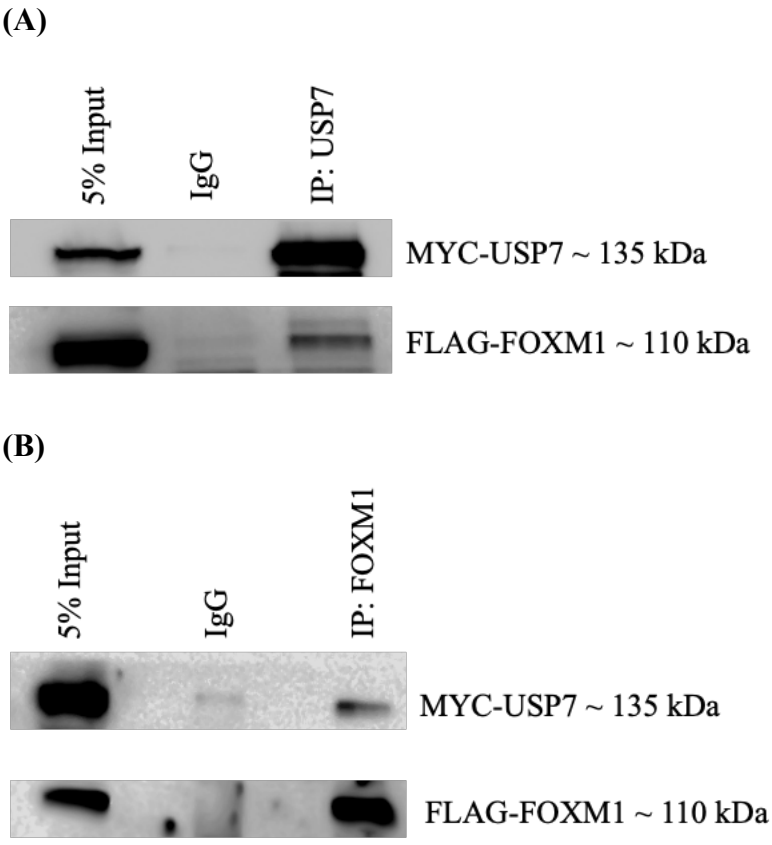

Figure 3.3. MYC-USP7 and FLAG-FOXM1 Interact *In Vivo*. U2OS whole cell lysates overexpressing both MYC-USP7 and FLAG-FOXM1 were immunoprecipitated with rabbit anti-USP7, (**A**) or rabbit anti-FOXM1, (**B**), using rabbit IgG as a negative control, followed by binding to Protein A/G beads. Immunoblotting was done using mouse anti-MYC, and mouse anti-FLAG antibodies.

3.2.3 The MYC-USP7 and FLAG-FOXM1 Interaction is Dependent on DWGF *In Vivo*

To determine whether it is indeed the ^{164}DWGF^{167} motif that is required for the interaction between FOXM1 and USP7 *in vivo*, co-immunoprecipitations were done with FLAG-FOXM1 and wild type MYC-USP7, as well as interaction site mutant MYC-USP7$^{DW\text{-}MRGR}$ (**Figure 3.4**). FLAG-FOXM1 was immunoprecipitated through M2 beads and the elution fractions were probed for MYC-USP7. FLAG-FOXM1 interacted with the wild type MYC-USP7 and exhibited a diminished interaction with MYC-USP7$^{DW\text{-}MRGR}$ as well as the empty vector pcDNA3.1/FLAG (**Figure 3.4**).

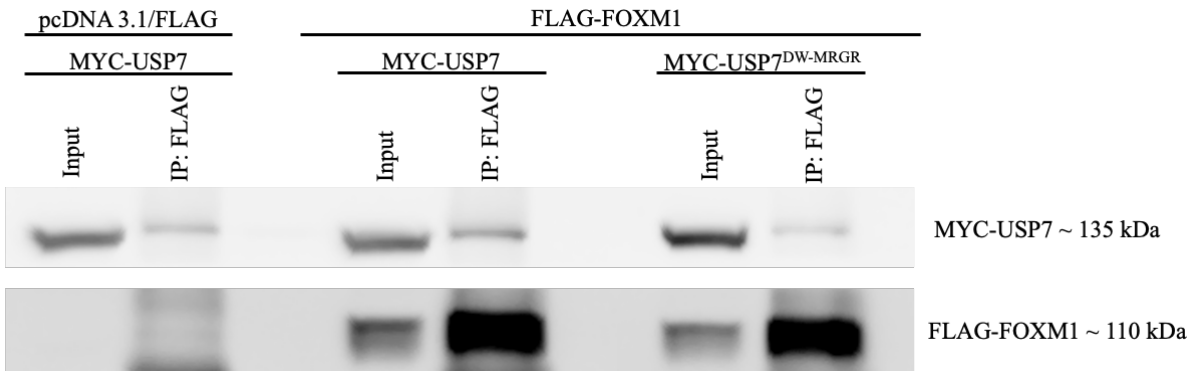

Figure 3.4. MYC-USP7 and FLAG-FOXM1 Interaction Depends on ^{164}DWGF^{167} *In Vivo*. U2OS cells transfected with 5 μg of pcDNA3.1/FLAG, and 5 μg MYC-USP7, as well as 5 μg of FLAG-FOXM1 with 5 μg of either MYC-USP7, or MYC-USP7$^{DW\text{-}MRGR}$. The cells were harvested after 48 hours, and anti-FLAG M2 Affinity Gel was used to immunoprecipitate FLAG-FOXM1. The inputs (5%) and elutions (10 μL) were resolved on a 7.5% SDS-PAGE gel, then transferred to a PVDF membrane. The membrane was blotted with mouse anti-FLAG, and anti-MYC mouse antibodies.

3.3 FOXM1 Interacts with the USP7 TRAF Domain via the ^{164}DWGF^{167} Motif *In Vitro*

To determine if it is indeed the ^{164}DWGF^{167} motif of the NTD of USP7 that interacts with FOXM1, a His-pulldown was done between FLAG FOXM1, with either the wild type 6x-His-USP7-NTD or the mutated 6x-His-USP7^{DW} NTD (**Figure 3.5**). U2OS cells exogenously expressing FLAG-FOXM1 were incubated with Nickel beads bound to either the purified wild type 6x-His-USP7-NTD or the 6x-His-USP7^{DW}-NTD (**Figure 3.5**). FLAG-FOXM1 appeared to bind tightly to the wild type 6x-His-USP7-NTD, though not to the empty Nickel beads, which served as the negative control, and FLAG-FOXM1 appeared to exhibit a diminished interaction with the mutant 6x-His-USP7^{DW}-NTD (**Figure 3.5**).

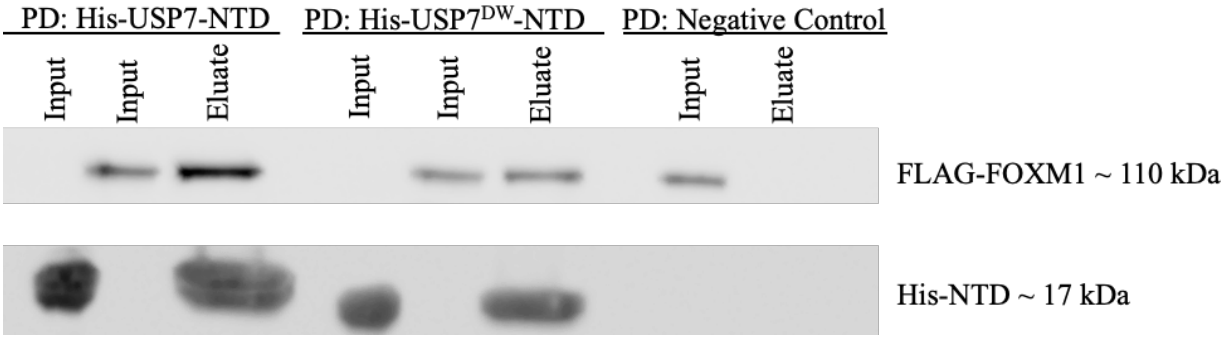

Figure 3.5. FLAG-FOXM1 Interacts with His-USP7 NTD via the ^{1647}DWGF^{167} Motif *In Vitro*. His-pulldown of FLAG-FOXM1 with wild type 6xHis-USP7-NTD and 6xHis-USP7^{DW}-NTD. FLAG-FOXM1 was incubated with beads bound to either wild type 6xHis-USP7-NTD, or 6xHis-USP7^{DW}-NTD. The input (5%) and elution (30 μL) fractions were resolved on a 12% SDS-PAGE gel, transferred to a PVDF membrane, then blotted with mouse anti-His and mouse anti-FLAG antibodies. PD: Pull Down.

3.4 USP7 Regulates FOXM1 Stability *In Vivo*

The impact of USP7 on the stability of FOXM1 was investigated through various *in vivo* assays including siRNA mediated knockdown of USP7, overexpression of wild type, and catalytically inactive USP7. Additional *in vivo* assays consisted of comparing FOXM1 levels in HCT116 parental versus HCT116 USP7$^{-/-}$ cells, and reconstitution of USP7 in HCT116 USP7$^{-/-}$ cells.

3.4.1 FOXM1 Levels Are Decreased in HCT116 USP7$^{-/-}$ Cells

The regulatory relationship between USP7 and FOXM1 was investigated through various assays. Endogenous FOXM1 levels were probed for in U2OS cells, as well as, in HCT116 parental cells, and HCT116 USP7$^{-/-}$ cells (**Figure 3.6**). FOXM1 was most abundant in U2OS and HCT116 parental cells, whereas in HCT116 USP7$^{-/-}$ cells FOXM1 was reduced (**Figure 3.6**).

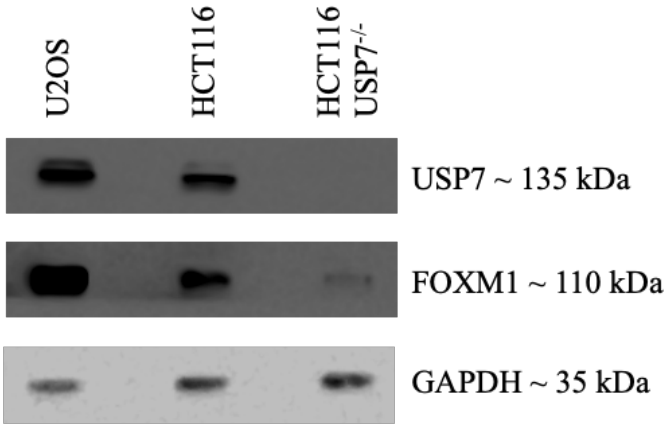

Figure 3.6. Endogenous Levels of USP7 and FOXM1 in U2OS, HCT116 parental, and in HCT116 USP7$^{-/-}$ cells. Whole cell lysates (20 ug) of U2OS, HCT116, and HCT116 USP7$^{-/-}$ cells were resolved on a 10% SDS-PAGE gel and transferred to a PVDF membrane. The membrane was blotted with mouse anti-USP7, rabbit anti-FOXM1 and mouse anti-GAPDH antibodies. n = 2.

3.4.2 Ectopic Expression of MYC-USP7 Increases FOXM1 Stability

To further investigate the impact of USP7 on the stability of FOXM1, HeLa cells were transfected with either empty vector pcDNA3/MYC, MYC-USP7, or catalytically inactive MYC-USP7^{C223S} (**Figure 3.7**). The HeLa cells expressing pcDNA3, or the catalytically inactive MYC-USP7^{C223S} exhibited similar levels of endogenous FOXM1, whereas the HeLa cells expressing wild type MYC-USP7 exhibited increased levels of endogenous FOXM1 (**Figure 3.7**).

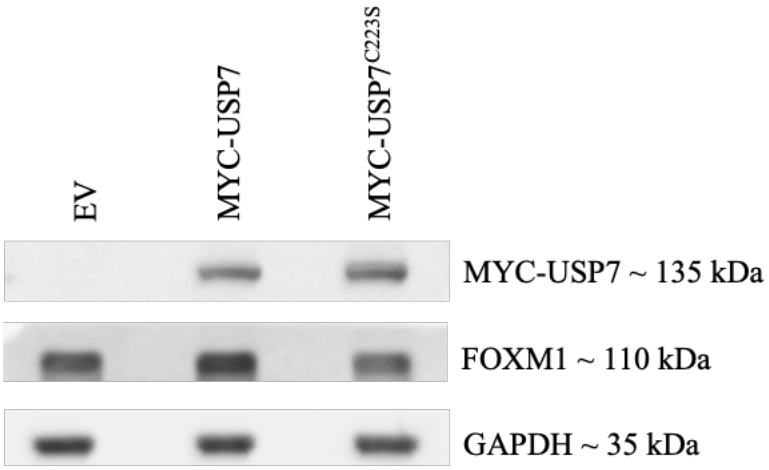

Figure 3.7. Overexpression of Wild Type MYC-USP7 Stabilises Endogenous Levels of FOXM1. Cell lysates (40 ug) of HeLa cells transfected with either empty vector (pcDNA3), wild type MYC-USP7 or MYC-USP7^{C223S} were resolved on a 10% SDS-PAGE gel and transferred to a PVDF membrane. The membrane was blotted with mouse anti-MYC, rabbit anti-FOXM1 and mouse anti-GAPDH antibodies. EV: empty vector, pcDNA3/MYC. n = 1.

3.4.3 FOXM1 Levels Increase Upon Reconstitution of MYC-USP7 in HCT116 USP7$^{-/-}$ Cells

In order to assess the impact of USP7 on FOXM1's stability further, USP7 was reconstituted in HCT116 USP7$^{-/-}$ cells. An empty vector control, pcDNA3/MYC, or MYC-USP7 was transfected into HCT116 USP7$^{-/-}$ cells (**Figure 3.8**). Upon expression of MYC-USP7, endogenous levels of FOXM1 increased compared to the empty vector control (**Figure 3.8**).

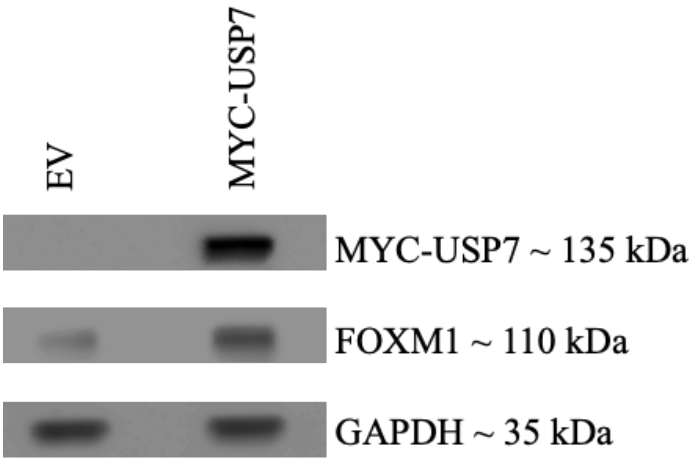

Figure 3.8. MYC- USP7 Reconstitution in HCT116 USP7$^{-/-}$ cells Stabilises FOXM1. HCT116 USP7$^{-/-}$ cells were transiently transfected with either pcDNA3/MYC (empty vector) or MYC-USP7 for 24 hours. Whole cell lysates (20 ug) were resolved on a 10% SDS-PAGE gel and transferred to a PVDF membrane. The membrane was blotted with mouse anti-USP7, rabbit anti-FOXM1, and mouse anti-GAPDH antibodies. EV: Empty Vector, pcDNA3/MYC. n =1.

3.4.4 siUSP7 Decreases FOXM1 Stability

USP7's impact on FOXM1's stability was also assessed through siRNA mediated knockdown of USP7 in HeLa cells (**Figure 3.9**). The levels of endogenous USP7 were noticeably decreased in HeLa cells transfected with siUSP7 for 96 hours, and the levels of endogenous FOXM1 decreased correspondingly (**Figure 3.9**).

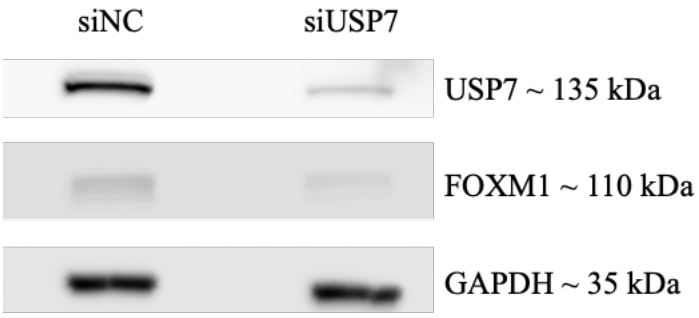

Figure 3.9. siRNA Mediated USP7 Knockdown Decreases Stability of Endogenous FOXM1. Whole cell lysates (40 ug) of HeLa cells transfected with either siNC or siUSP7 for 96 hours were resolved on a 10% SDS-PAGE gel and transferred to a PVDF membrane. The membrane was blotted with mouse anti-USP7, rabbit anti-FOXM1, and mouse anti-GAPDH antibodies. n =2.

CHAPTER 4: DISCUSSION AND CONCLUSION

The objective of this thesis project was to identify if USP7 interacts with FOXM1, and subsequently regulates FOXM1 stability. This interaction was hypothesized to occur *in vitro*, as well as *in vivo*, as FOXM1 contains many (P/A/E)xxS sequences, which have been shown to facilitate interaction between USP7 and previously identified substrates, via the ^{164}DWGF^{167} motif in the TRAF domain at the NTD of USP7. This interaction was hypothesized to impact the stability of FOXM1 in mammalian cell lines via deubiquitination by USP7.

4.1 USP7 Regulates Stability of FOXM1

Seeing as USP7's most distinguished role in the cell is to deubiquitinate substrates therefore preventing degradation by the 26S proteasome, which has been shown to regulate the stability of its substrates, for example EZH2, it was hypothesized that FOXM1's stability may also be regulated by USP7 (Gagarina et al, 2019). To explore the impact of inhibiting the proteasome on FOXM1, HCT116 parental and HCT116 USP7$^{-/-}$ cells were treated with MG-132, a well-known proteasome inhibitor, and DMSO, as a control for 2 hours. The levels of FOXM1 increased in both cell lines when treated with MG-132, providing support for the role of the proteasome in the stability of FOXM1 in cells (**Figure 3.1**). The levels of FOXM1 increased in HCT116 USP7$^{-/-}$ cells were treated with MG-132 compared to the control, suggesting that without USP7 present for deubiquitination, FOXM1 would be degraded by the proteasome, and subsequently would not be as stable (**Figure 3.1**). This finding shows that inhibition of the proteasome prevents FOXM1 degradation. This finding supports previous research which showed that FOXM1 levels are stabilised upon MG-132 treatment, therefore FOXM1 stability is mediated by the ubiquitin proteasome system (Li et al, 2017; Chen et al, 2016; Chen et al, 2021).

To explore the impact of USP7 on FOXM1 levels, U2OS, HCT116 parental, and HCT116 USP7$^{-/-}$ cells were compared. FOXM1 was not as highly expressed in HCT116 USP7$^{-/-}$ cells compared to HCT116 parental, and U2OS cells, indicating that FOXM1 stability is dependent on the presence of USP7 (**Figure 3.6**). This finding corresponds to previous research which has shown that in cells treated with increasing concentrations of the deubiquitinase inhibitor PR-619, FOXM1 levels decreased, therefore degradation of FOXM1 can be prevented by deubiquitinases (Arceci et al, 2019). As USP7 affects the level of FOXM1 in cells, wild type MYC-USP7's overexpression in HeLa cells leads to an increase in stability of FOXM1 compared to the overexpression of the catalytically inactive mutant MYC-USP7^{C223S} (**Figure 3.7**). This finding suggests that the catalytic domain of USP7 is essential for regulating the stability of FOXM1 in cells. The catalytic domain of USP7 is responsible for deubiquitination of substrates which is expected to increase substrate stability, therefore this finding insinuates that USP7 positively regulates FOXM1 via deubiquitination (Pozhidaeva & Bezsonova, 2019). This finding is similar to previous research that showed that overexpression of wild type USP28 leads to increased levels of FOXM1, supporting the idea that USP28 positively regulates FOXM1 levels (Chen et al, 2021). Since in HCT USP7$^{-/-}$ cells, there is less FOXM1 compared to HCT parental cells, the regulatory relationship between USP7, and FOXM1 was further explored by introducing wild type MYC-USP7 in HCT USP7$^{-/-}$ cells. Upon ectopic expression of wild type MYC-USP7 in HCT USP7$^{-/-}$ cells, FOXM1 levels increased compared to the empty vector control, providing more evidence that USP7 does increase stability of FOXM1, which is presumed to be due to the deubiquitinase activity of USP7 (**Figure 3.8**). Knockdown of USP7 via siRNA in HeLa cells showed that a decrease in USP7 lead to a corresponding decrease in FOXM1 levels compared to the negative control, further demonstrating that USP7 levels impact

FOXM1 levels (**Figure 3.9**). This finding is also similar to previous findings that upon siRNA mediated knockdown of USP21 and USP22, as well as knockdown of USP28, and USP5 via shRNA, FOXM1 levels decreased as well (Arceci et al, 2019; Ning et al, 2014: Chen et al, 2021; Li et al, 2017).

4.2 USP7 Interacts with FOXM1 via the NTD ^{164}DWGF^{167} Motif of USP7

The investigation into the interaction between USP7 and FOXM1 was conducted through various pull-down assays. An endogenous immunoprecipitation was conducted to observe whether the interaction between USP7 and FOXM1 was occurring innately. Indeed, FOXM1 was endogenously co-immunoprecipitated with USP7 *in vivo* (**Figure 3.2**). A co-immunoprecipitation assay using whole cell lysates of U2OS exogenously expressing MYC-USP7, and FLAG-FOXM1 confirmed interaction between MYC-USP7, and FLAG-FOXM1 *in vivo*, as can be seen in the reciprocal co-immunoprecipitation assays (**Figure 3.3**). This *in vivo* interaction is presumed to be occurring through the (P/A/E)xxS motifs of FLAG-FOXM1 interacting with the ^{164}DWGF^{167} motif in the TRAF domain at the NTD of MYC- USP7.

In order to determine if it is indeed the ^{164}DWGF^{167} motif in the TRAF domain at the NTD of MYC- USP7 that is responsible for the *in vivo* interaction seen with FLAG-FOXM1, co-immunoprecipitations were conducted using an interaction site mutant of MYC-USP7. Cells co-expressing FLAG-FOXM1, and MYC-USP7 or MYC-USP7$^{DW\text{-}MRGR}$ mutant were used and FLAG-FOXM1 was immunoprecipitated. Wild type MYC-USP7 co-immunoprecipitated strongly with FLAG-FOXM1, in comparison the MYC-USP7$^{DW\text{-}MRGR}$ mutant did not interact as well with FLAG-FOXM1 (**Figure 3.4**). This immunoprecipitation demonstrated that the ^{164}DWGF^{167} motif of USP7 is essential for the *in vivo* interaction between USP7, and FOXM1.

To verify that it is the ^{164}DWGF^{167} motif that is responsible for interaction between USP7 and FOXM1, an *in vitro* His pull-down assay was conducted using purified wild type 6x-His-USP7-NTD, and 6x-His-USP7^{DW}-NTD. The 6x-His-USP7^{DW}-NTD is mutated such that the aspartic acid and tryptophan residues are mutated to alanine. FLAG-FOXM1 interacted strongly with the purified 6x-His-USP7-NTD, compared to the 6x-His-USP7^{DW}-NTD, indicating that the aspartic acid and tryptophan residues of the ^{164}DWGF^{167} motif of USP7's NTD are necessary for the interaction with FOXM1 (**Figure 3.5)**. This result is in agreement with previous findings that emphasize the importance of the aspartate and tryptophan residues in the ^{164}DWGF^{167} motif of the TRAF domain of USP7 to interact with substrates p53, MDM2, and EBNA1 (Sheng et al, 2006). This finding provides support for the hypothesis that FOXM1 interacts specifically through the ^{164}DWGF^{167} motif at the NTD domain of USP7, similarly to previously identified substrates that also contain (P/A/E)xxS consensus sequences, such as, vIRF1, EBNA1, and MDM2 (Chavoshi et al, 2016; Saridakis et al, 2005; Sheng et al, 2006).

4.3 Implications of USP7 and FOXM1 Interaction in Cellular Proliferation

The interaction between USP7, and FOXM1 has elucidated a novel manner in which USP7 may be involved in cellular proliferation. It is well known that FOXM1 expression varies depending on the cell cycle, based on the aforementioned findings USP7 interacts with FOXM1 and has a role in FOXM1's stability, therefore it is possible USP7 helps regulate progression through the cell cycle through its interaction with FOXM1.

One of the pathways essential for regulating expression of genes needed to progress through the cell cycle is the Wnt/β-catenin signalling pathway in which the transcription factor β-catenin activates expression of genes such as c-MYC, and cyclin D1 (Moon et al, 2014). FOXM1, like USP7 is implicated in cell cycle progression, as well as the Wnt/β-catenin

signalling pathway. FOXM1 has been implicated in β-catenin nuclear translocation and was found to interact with β-catenin in order to bind to WREs to initiate transcription of genes needed for cell cycle progression (Chen et al, 2016; Zhang et al, 2011). USP7 was found to interact with β-catenin via its TRAF domain and increase stability of β-catenin leading to the activation of Wnt/β-catenin signalling pathway (Ma et al, 2014; Novellasdemunt et al, 2017; Zhu et al, 2020). Wnt treatment of cells results in a decrease FOXM1 degradation through inhibition of FOXM1 degradation by USP5, it is possible that upon activation of the Wnt//β-catenin signalling pathway FOXM1 may be protected from proteasomal degradation by USP7 as well (Chen et al, 2016). Previous research showed that various USPs can increase FOXM1 stability, which can lead to increased stability and nuclear localization of β-catenin, culminating in FOXM1 complexed with β-catenin on WREs in order to activate expression of Wnt target genes, resulting in cell cycle progression (Chen et al, 2016; Chen et al, 2021; Li et al, 2017; Ning et al, 2014; Zhang et al, 2011). USP7 is known to be a positive regulator of the Wnt/β-catenin signalling pathway, it would be interesting to further investigate the relationship between USP7 and FOXM1 to determine if this interaction is instrumental in the Wnt/β-catenin signalling pathway.

Plk1 is involved in phosphorylating FOXM1 to conformationally change the FOXM1 structure resulting in the activation of FOXM1 (Marceau et al, 2019). USP7 interacts with Plk1 to stabilise it, and without USP7, Plk1 is degraded (Peng et al, 2019). The USP7 inhibitor P5091 promotes degradation of Plk1, slows cell proliferation, and induces cellular apoptosis (Peng et al, 2019). It is plausible that USP7 stabilising Plk1 results in FOXM1 activation, and the active FOXM1 may be stabilised by USP7 as well. This could be studied by investigating via *in vivo* stability studies looking at USP7, Plk1, and FOXM1 levels, upon ectopic expression of USP7 as

well as upon siRNA mediated knockdown of USP7. P5091 also prevents USP7 from deubiquitinating β-catenin leading to degradation of β-catenin, culminating in Wnt/β-catenin pathway inactivation, therefore inhibiting colorectal tumour growth *in vivo* (An et al, 2017). It is also possible that USP7 inhibition combined with Plk1 degradation may destabilise FOXM1, and may prevent β-catenin nuclear accumulation, therefore contributing to the decreased cellular proliferation seen upon P5091 treatment. Along with P5091's already proven function in promoting Plk1 and β-catenin degradation, it would be interesting to see if P5091 could also inhibit USP7's stabilisation of FOXM1, and if that consequently causes a reduction in cell proliferation through an MTS assay as well as *in vivo* tumour growth assay.

4.4 Future Directions

To verify that USP7 is indeed deubiquitinating FOXM1, an *in vivo* deubiquitination assay could be done involving the wild type MYC-USP7 and the catalytically inactive MYC-USP7^{C223S}, similar work was done with a catalytically inactive mutant of USP21 which showed increased polyubiquitination of FOXM1 upon expression of catalytically inactive USP21 (Arceci et al, 2019). A comparison between the amount of polyubiquitinated FOXM1 in siNC versus siUSP7 cells could also be conducted, such as was done for USP28 which showed increased polyubiquitinated FOXM1 upon expression of siUSP28 and simultaneous MG-132 treatment (Chen et al, 2021). To assess the impact of the USP7 and FOXM1 interaction on the Wnt/β-catenin signalling pathway, it would be of interest to assess the effect of loss of USP7 on the transcriptional activity of FOXM1 and Wnt target genes. It is possible for qRT-PCR to be used to examine the mRNA levels of FOXM1 and Wnt transcriptional targets to see if silencing USP7 reduces transcriptional activity of Wnt target genes, as well as if silencing USP7 causes a reduction in transcriptional activity of FOXM1 in the same way that silencing USP21 reduces

FOXM1 transcriptional activity (Arceci et al, 2019). It would be of interest to also analyse the abundance of Wnt transcriptional targets in cells using western blots to determine if *in vivo* USP7 regulates proteins expressed upon Wnt/β-catenin signalling pathway activation, such as c-MYC, cyclin D1 and VEGF, in a similar manner to USP28 (Chen et al, 2021). A more detailed investigation of the interaction between USP7 and FOXM1 may clarify the implications of this interaction *in vivo*.

A recent study suggested the identification of allosteric binding sites to inhibit USP7 since the catalytic domain of USPs are homologous which may lead to off target effects (Li & Liu, 2020). Developing novel USP7 inhibitors that may target its interaction with substrates may be beneficial as USPs have diverse amino acid sequences in their non-catalytic domains that confer substrate specificity (Pfoh et al, 2015a). Both USP7, and FOXM1 overexpression have been implicated in a variety of cancers, especially colorectal cancer that exhibits hyperactive Wnt/β-catenin signalling pathway due to mutated APC or β-catenin (An et al, 2017; Laissue, 2019). The USP7 inhibitor P5091 was found to inhibit USP7 mediated deubiquitination of β-catenin leading to inactivation of the Wnt/β-catenin signalling pathway (An et al, 2017). Targeting the interaction between USP7 and FOXM1 may represent a novel way to inhibit aberrant cellular proliferation due to overactivation of the Wnt/β-catenin signalling pathway. FOXM1 is an ideal cancer therapeutic target because of its high expression in proliferative cancer cells, and it is essential for β-catenin nuclear localization, therefore increasing its proteasomal degradation may decrease its oncogenic effect (Zhang et al, 2011). Destabilisation of FOXM1 through USP7 inhibition may be a promising route to downregulate FOXM1 stability in cancer cells. Therefore, it is of interest to better characterize the interaction between USP7 and FOXM1 in order to elucidate whether targeting this interaction may be a novel way to prevent

aberrant activation of Wnt/β-catenin signalling, and consequently prevent the abnormal expression of genes that enable cellular proliferation.

4.5 Conclusion

The ^{164}DWGF^{167} motif in the TRAF domain at the NTD of USP7 is known to facilitate interaction with USP7 substrates that contain (P/A/E)xxS sequences, therefore upon realizing that FOXM1 contains many of these sequences, it was hypothesized that FOXM1 is a potential substrate of USP7. Indeed, FOXM1 is shown to interact with USP7 via the ^{164}DWGF^{167} motif *in vivo*, and *in vitro*, providing support for FOXM1 as a newly identified interacting partner of USP7. FOXM1 levels were attenuated in response to overexpression, and knockdown of USP7, which is believed to be occurring via the role of USP7 as a deubiquitinase. Overall, the interaction between USP7 and FOXM1 has introduced a novel manner in which USP7 may contribute to the process of cellular proliferation, which if improperly regulated may lead to tumourigenesis.

REFERENCES

1. Adhikari, A., Xu, M., & Chen, Z. J. (2007). Ubiquitin-mediated activation of TAK1 and IKK. *Oncogene*, *26*(22), 3214–3226. https://doi-org/10.1038/sj.onc.1210413
2. Akutsu, M., Dikic, I., & Bremm, A. (2016). Ubiquitin chain diversity at a glance. *Journal Of Cell Science*, *129*(5), 875–880. https://doi-org/10.1242/jcs.183954
3. Amerik, A. Y., & Hochstrasser, M. (2004). Mechanism and function of deubiquitinating enzymes. *Biochimica et Biophysica Acta*, *1695*(1-3), 189–207. https://doi-org/10.1016/j.bbamcr.2004.10.003
4. An, T., Gong, Y., Li, X., Kong, L., Ma, P., Gong, L., Zhu, H., Yu, C., Liu, J., Zhou, H., Mao, B., & Li, Y. (2017). USP7 inhibitor P5091 inhibits Wnt signaling and colorectal tumor growth. *Biochemical Pharmacology*, *131*, 29–39. https://doi-org/10.1016/j.bcp.2017.02.011
5. Arceci, A., Bonacci, T., Wang, X., Stewart, K., Damrauer, J. S., Hoadley, K. A., & Emanuele, M. J. (2019). FOXM1 Deubiquitination by USP21 Regulates Cell Cycle Progression and Paclitaxel Sensitivity in Basal-like Breast Cancer. *Cell Reports*, *26*(11), 3076-3086.e6. https://doi.org/10.1016/j.celrep.2019.02.054
6. Bhattacharya, S., & Ghosh, M. K. (2014). HAUSP, a novel deubiquitinase for Rb - MDM2 the critical regulator. *The FEBS Journal*, *281*(13), 3061–3078. https://doi-org/10.1111/febs.12843
7. Bojagora, A., & Saridakis, V. (2020, September 1). USP7 manipulation by viral proteins. *Virus Research*. Elsevier B.V. https://doi.org/10.1016/j.virusres.2020.198076

8. Bonacci, T., & Emanuele, M. J. (2020). Dissenting degradation: Deubiquitinases in cell cycle and cancer. *Seminars in Cancer Biology*, *67*(Pt 2), 145–158. https://doi-org/10.1016/j.semcancer.2020.03.008
9. Chan, N. L., & Hill, C. P. (2001). Defining polyubiquitin chain topology. *Nature Structural Biology*. https://doi.org/10.1038/90337
10. Chauhan, D., Tian, Z., Nicholson, B., Kumar, K. G., Zhou, B., Carrasco, R., McDermott, J. L., Leach, C. A., Fulcinniti, M., Kodrasov, M. P., Weinstock, J., Kingsbury, W. D., Hideshima, T., Shah, P. K., Minvielle, S., Altun, M., Kessler, B. M., Orlowski, R., Richardson, P., Munshi, N., … Anderson, K. C. (2012). A small molecule inhibitor of ubiquitin-specific protease-7 induces apoptosis in multiple myeloma cells and overcomes bortezomib resistance. *Cancer Cell*, *22*(3), 345–358. https://doi-org/10.1016/j.ccr.2012.08.007
11. Chavoshi, S., Egorova, O., Lacdao, I. K., Farhadi, S., Sheng, Y., & Saridakis, V. (2016). Identification of Kaposi Sarcoma Herpesvirus (KSHV) vIRF1 Protein as a Novel Interaction Partner of Human Deubiquitinase USP7. *The Journal of Biological Chemistry*, *291*(12), 6281–6291. https://doi-org/10.1074/jbc.M115.710632
12. Chen, L., Xu, Z., Li, Q., Feng, Q., Zheng, C., Du, Y., Yuan, R., & Peng, X. (2021). USP28 facilitates pancreatic cancer progression through activation of Wnt/β-catenin pathway via stabilising FOXM1. *Cell Death & Disease*, *12*(10), 887. https://doi-org/10.1038/s41419-021-04163-z
13. Chen, Y., Li, Y., Xue, J., Gong, A., Yu, G., Zhou, A., … Huang, S. (2016). Wnt-induced deubiquitination FoxM1 ensures nucleus β-catenin transactivation. *The EMBO Journal*, *35*(6), 668–684. https://doi.org/10.15252/embj.201592810

14. Clevers, H., & Nusse, R. (2012). Wnt/β-catenin signaling and disease. *Cell*, *149*(6), 1192–1205. https://doi-org/10.1016/j.cell.2012.05.012

15. Daniels, D. L., & Weis, W. I. (2002). ICAT inhibits beta-catenin binding to Tcf/Lef-family transcription factors and the general coactivator p300 using independent structural modules. *Molecular Cell*, *10*(3), 573–584. https://doi-org/10.1016/s1097-2765(02)00631-7

16. Dwane, L., Gallagher, W. M., Ní Chonghaile, T., & O'Connor, D. P. (2017). The Emerging Role of Non-traditional Ubiquitination in Oncogenic Pathways. *The Journal of Biological Chemistry*, *292*(9), 3543–3551. https://doi-org/10.1074/jbc.R116.755694

17. Faesen, A. C., Dirac, A. M., Shanmugham, A., Ovaa, H., Perrakis, A., & Sixma, T. K. (2011). Mechanism of USP7/HAUSP activation by its C-terminal ubiquitin-like domain and allosteric regulation by GMP-synthetase. *Molecular Cell*, *44*(1), 147–159. https://doi-org/10.1016/j.molcel.2011.06.034

18. Fang, S., & Weissman, A. M. (2004). A field guide to ubiquitylation. *Cellular and Molecular Life Sciences: CMLS*, *61*(13), 1546–1561. https://doi-org/10.1007/s00018-004-4129-5

19. Fountain, M. D., Oleson, D. S., Rech, M. E., Segebrecht, L., Hunter, J. V., McCarthy, J. M., Lupo, P. J., Holtgrewe, M., Moran, R., Rosenfeld, J. A., Isidor, B., Le Caignec, C., Saenz, M. S., Pedersen, R. C., Morgan, T. M., Pfotenhauer, J. P., Xia, F., Bi, W., Kang, S. L., Patel, A., … Schaaf, C. P. (2019). Pathogenic variants in USP7 cause a neurodevelopmental disorder with speech delays, altered behavior, and neurologic anomalies. *Genetics in Medicine: Official Journal of the American College of Medical Genetics*, *21*(8), 1797–1807. https://doi-org/10.1038/s41436-019-0433-1

20. Gagarina, V., Bojagora, A., Lacdao, I. K., Luthra, N., Pfoh, R., Mohseni, S., … Saridakis, V. (2020). Structural Basis of the Interaction Between Ubiquitin Specific Protease 7 and Enhancer of Zeste Homolog 2. *Journal of Molecular Biology*, *432*(4), 897–912. https://doi.org/10.1016/j.jmb.2019.12.026

21. Georges, A., Coyaud, E., Marcon, E., Greenblatt, J., Raught, B., & Frappier, L. (2019). USP7 Regulates Cytokinesis through FBXO38 and KIF20B. *Scientific Reports*, *9*(1), 2724. https://doi-org/10.1038/s41598-019-39368-y

22. Giovinazzi, S., Sirleto, P., Aksenova, V., Morozov, V. M., Zori, R., Reinhold, W. C., & Ishov, A. M. (2014). Usp7 protects genomic stability by regulating Bub3. *Oncotarget*, *5*(11), 3728–3742. https://doi-org/10.18632/oncotarget.1989

23. Graham, T. A., Clements, W. K., Kimelman, D., & Xu, W. (2002). The crystal structure of the beta-catenin/ICAT complex reveals the inhibitory mechanism of ICAT. *Molecular Cell*, *10*(3), 563–571. https://doi-org/10.1016/s1097-2765(02)00637-8

24. Grice, G. L., & Nathan, J. A. (2016). The recognition of ubiquitinated proteins by the proteasome. *Cellular and Molecular Life Sciences: CMLS*, *73*(18), 3497–3506. https://doi-org/10.1007/s00018-016-2255-5

25. Halasi, M., & Gartel, A. L. (2013). FOX(M1) news--it is cancer. *Molecular Cancer Therapeutics*, *12*(3), 245–254. https://doi-org/10.1158/1535-7163.MCT-12-0712

26. Hershko, A., & Ciechanover, A. (1998). The ubiquitin system. *Annual Review of Biochemistry*. https://doi.org/10.1146/annurev.biochem.67.1.425

27. Hoege, C., Pfander, B., Moldovan, G. L., Pyrowolakis, G., & Jentsch, S. (2002). RAD6-dependent DNA repair is linked to modification of PCNA by ubiquitin and SUMO. *Nature*, *419*(6903), 135–141. https://doi-org/10.1038/nature00991

28. Hu, M., Li, P., Li, M., Li, W., Yao, T., Wu, J. W., Gu, W., Cohen, R. E., & Shi, Y. (2002). Crystal structure of a UBP-family deubiquitinating enzyme in isolation and in complex with ubiquitin aldehyde. *Cell*, *111*(7), 1041–1054. https://doi-org/10.1016/s0092-8674(02)01199-6

29. Kalathil, D., John, S., & Nair, A. S. (2021). FOXM1 and Cancer: Faulty Cellular Signaling Derails Homeostasis. *Frontiers in Oncology*, *10*, 626836. https://doi-org/10.3389/fonc.2020.626836

30. Kang, D., Chen, J., Wong, J., & Fang, G. (2002). The checkpoint protein Chfr is a ligase that ubiquitinates Plk1 and inhibits Cdc2 at the G2 to M transition. *The Journal of Cell Biology*, *156*(2), 249–259. https://doi-org/10.1083/jcb.200108016

31. Komander, D., Clague, M. J., & Urbé, S. (2009, August). Breaking the chains: Structure and function of the deubiquitinases. *Nature Reviews Molecular Cell Biology*. https://doi.org/10.1038/nrm2731

32. Komander, D., & Rape, M. (2012). The ubiquitin code. *Annual Review of Biochemistry*, *81*, 203–229. https://doi-org /10.1146/annurev-biochem-060310-170328

33. Kon, N., Kobayashi, Y., Li, M., Brooks, C. L., Ludwig, T., & Gu, W. (2010). Inactivation of HAUSP in vivo modulates p53 function. *Oncogene*, *29*(9), 1270–1279. https://doi-org/10.1038/onc.2009.427

34. Koo, C. Y., Muir, K. W., & Lam, E. W. (2012). FOXM1: From cancer initiation to progression and treatment. *Biochimica et Biophysica Acta*, *1819*(1), 28–37. https://doi-org/10.1016/j.bbagrm.2011.09.004

35. Laissue P. (2019). The forkhead-box family of transcription factors: key molecular players in colorectal cancer pathogenesis. *Molecular Cancer*, *18*(1), 5. https://doi-org/10.1186/s12943-019-0938-x

36. Laoukili, J., Alvarez, M., Meijer, L. A., Stahl, M., Mohammed, S., Kleij, L., Heck, A. J., & Medema, R. H. (2008). Activation of FoxM1 during G2 requires cyclin A/Cdk-dependent relief of autorepression by the FoxM1 N-terminal domain. *Molecular and Cellular Biology*, *28*(9), 3076–3087. https://doi-org/10.1128/MCB.01710-07

37. Laoukili, J., Kooistra, M. R., Brás, A., Kauw, J., Kerkhoven, R. M., Morrison, A., Clevers, H., & Medema, R. H. (2005). FoxM1 is required for execution of the mitotic programme and chromosome stability. *Nature Cell Biology*, *7*(2), 126–136. https://doi-org/10.1038/ncb1217

38. Laoukili, J., Stahl, M., & Medema, R. H. (2007, January). FoxM1: At the crossroads of ageing and cancer. *Biochimica et Biophysica Acta - Reviews on Cancer*. https://doi.org/10.1016/j.bbcan.2006.08.006

39. Leung, T. W., Lin, S. S., Tsang, A. C., Tong, C. S., Ching, J. C., Leung, W. Y., Gimlich, R., Wong, G. G., & Yao, K. M. (2001). Over-expression of FoxM1 stimulates cyclin B1 expression. *FEBS Letters*, *507*(1), 59–66. https://doi-org/10.1016/s0014-5793(01)02915-5

40. Li, M., Brooks, C. L., Kon, N., & Gu, W. (2004). A dynamic role of HAUSP in the p53-Mdm2 pathway. *Molecular Cell*, *13*(6), 879–886. https://doi-org/10.1016/s1097-2765(04)00157-1

41. Li, P., & Liu, H. M. (2020). Recent advances in the development of ubiquitin-specific-processing protease 7 (USP7) inhibitors. *European Journal of Medicinal Chemistry*, *191*, 112107. https://doi-org/10.1016/j.ejmech.2020.112107

42. Li, X. Y., Wu, H. Y., Mao, X. F., Jiang, L. X., & Wang, Y. X. (2017). USP5 promotes tumorigenesis and progression of pancreatic cancer by stabilizing FoxM1 protein. *Biochemical and Biophysical Research Communications*, *492*(1), 48–54. https://doi-org/10.1016/j.bbrc.2017.08.040

43. Li, Y., Guo, H., Wang, Z., Bu, H., Wang, S., Wang, H., Fang, H., Liu, Z., & Kong, B. (2020). Cyclin F and KIF20A, FOXM1 target genes, increase proliferation and invasion of ovarian cancer cells. *Experimental Cell Research*, *395*(2), 112212. https://doi-org/10.1016/j.yexcr.2020.112212

44. Liao, G. B., Li, X. Z., Zeng, S., Liu, C., Yang, S. M., Yang, L., … Bai, J. Y. (2018, September 12). Regulation of the master regulator FOXM1 in cancer. *Cell Communication and Signaling*. BioMed Central Ltd. https://doi.org/10.1186/s12964-018-0266-6

45. Liu, C., Barger, C. J., & Karpf, A. R. (2021). FOXM1: A Multifunctional Oncoprotein and Emerging Therapeutic Target in Ovarian Cancer. *Cancers*, *13*(12), 3065. https://doi-org/10.3390/cancers13123065

46. Liu, P., Gan, W., Su, S., Hauenstein, A. V., Fu, T. M., Brasher, B., Schwerdtfeger, C., Liang, A. C., Xu, M., & Wei, W. (2018). K63-linked polyubiquitin chains bind to DNA to facilitate DNA damage repair. *Science Signaling*, *11*(533), eaar8133. https://doi-org/10.1126/scisignal.aar8133

47. Ma, P., Yang, X., Kong, Q., Li, C., Yang, S., Li, Y., & Mao, B. (2014). The ubiquitin ligase RNF220 enhances canonical Wnt signaling through USP7-mediated deubiquitination of β-catenin. *Molecular and Cellular Biology*, *34*(23), 4355–4366. https://doi-org/10.1128/MCB.00731-14

48. Mansour, M. A. (2018). Ubiquitination: Friend and foe in cancer. *International Journal of Biochemistry and Cell Biology*. Elsevier Ltd. https://doi.org/10.1016/j.biocel.2018.06.001

49. Marceau, A. H., Brison, C. M., Nerli, S., Arsenault, H. E., McShan, A. C., Chen, E., … Rubin, S. M. (2019). An order-to-disorder structural switch activates the foxm1 transcription factor. *ELife*, *8*. https://doi.org/10.7554/eLife.46131

50. Mevissen, T., & Komander, D. (2017). Mechanisms of Deubiquitinase Specificity and Regulation. *Annual Review of Biochemistry*, *86*, 159–192. https://doi-org/10.1146/annurev-biochem-061516-044916

51. Meyer, H. J., & Rape, M. (2014). Enhanced protein degradation by branched ubiquitin chains. *Cell*, *157*(4), 910–921. https://doi-org/10.1016/j.cell.2014.03.037

52. Moon, R. T., Kohn, A. D., De Ferrari, G. V., & Kaykas, A. (2004). WNT and beta-catenin signalling: diseases and therapies. *Nature Reviews. Genetics*, *5*(9), 691–701. https://doi-org/10.1038/nrg1427

53. Nakajima, S., Lan, L., Wei, L., Hsieh, C. L., Rapić-Otrin, V., Yasui, A., & Levine, A. S. (2014). Ubiquitin-specific protease 5 is required for the efficient repair of DNA double-strand breaks. *PloS One*, *9*(1), e84899. https://doi-org/10.1371/journal.pone.0084899

54. Nandi, D., Cheema, P. S., Jaiswal, N., & Nag, A. (2018, October 1). FoxM1: Repurposing an oncogene as a biomarker. *Seminars in Cancer Biology*. Academic Press. https://doi.org/10.1016/j.semcancer.2017.08.009

55. Nijman, S. M., Luna-Vargas, M. P., Velds, A., Brummelkamp, T. R., Dirac, A. M., Sixma, T. K., & Bernards, R. (2005). A genomic and functional inventory of deubiquitinating enzymes. *Cell*, *123*(5), 773–786. https://doi-org/10.1016/j.cell.2005.11.007

56. Ning, Z., Wang, A., Liang, J., Xie, Y., Liu, J., Feng, L., Yan, Q., & Wang, Z. (2014). USP22 promotes the G1/S phase transition by upregulating FoxM1 expression via β-catenin nuclear localization and is associated with poor prognosis in stage II pancreatic ductal adenocarcinoma. *International Journal of Oncology*, *45*(4), 1594–1608. https://doi-org /10.3892/ijo.2014.2531

57. Novellasdemunt, L., Foglizzo, V., Cuadrado, L., Antas, P., Kucharska, A., Encheva, V., Snijders, A. P., & Li, V. (2017). USP7 Is a Tumor-Specific WNT Activator for APC-Mutated Colorectal Cancer by Mediating β-Catenin Deubiquitination. *Cell Reports*, *21*(3), 612–627. https://doi-org/10.1016/j.celrep.2017.09.072

58. Nusse, R., & Clevers, H. (2017). Wnt/β-Catenin Signaling, Disease, and Emerging Therapeutic Modalities. *Cell*, *169*(6), 985–999. https://doi-org/10.1016/j.cell.2017.05.016

59. Oh, Y. M., Yoo, S. J., & Seol, J. H. (2007). Deubiquitination of Chfr, a checkpoint protein, by USP7/HAUSP regulates its stability and activity. *Biochemical and Biophysical Research Communications*, *357*(3), 615–619. https://doi-org/10.1016/j.bbrc.2007.03.193

60. Pandit, B., Halasi, M., & Gartel, A. L. (2009). p53 negatively regulates expression of FoxM1. *Cell Cycle (Georgetown, Tex.)*, *8*(20), 3425–3427. https://doi-org/10.4161/cc.8.20.9628

61. Park, H. J., Costa, R. H., Lau, L. F., Tyner, A. L., & Raychaudhuri, P. (2008). Anaphase-promoting complex/cyclosome-CDH1-mediated proteolysis of the forkhead box M1 transcription factor is critical for regulated entry into S phase. *Molecular and Cellular Biology*, *28*(17), 5162–5171. https://doi-org/10.1128/MCB.00387-08

62. Peng, Y., Liu, Y., Gao, Y., Yuan, B., Qi, X., Fu, Y., Zhu, Q., Cao, T., Zhang, S., Yin, L., & Li, X. (2019). USP7 is a novel Deubiquitinase sustaining PLK1 protein stability and regulating chromosome alignment in mitosis. *Journal of Experimental & Clinical Cancer Research: CR*, *38*(1), 468. https://doi-org/10.1186/s13046-019-1457-8

63. Pfoh, R., Lacdao, I. K., & Saridakis, V. (2015, February 1). (a) Deubiquitinases and the new therapeutic opportunities offered to cancer. *Endocrine-Related Cancer*. BioScientifica Ltd. https://doi.org/10.1530/ERC-14-0516

64. Pfoh, R., Lacdao, I. K., Georges, A. A., Capar, A., Zheng, H., Frappier, L., & Saridakis, V. (2015). (b) Crystal Structure of USP7 Ubiquitin-like Domains with an ICP0 Peptide Reveals a Novel Mechanism Used by Viral and Cellular Proteins to Target USP7. *PLoS Pathogens*, *11*(6). https://doi.org/10.1371/journal.ppat.1004950

65. Pozhidaeva, A., & Bezsonova, I. (2019, April 1). USP7: Structure, substrate specificity, and inhibition. *DNA Repair*. Elsevier B.V. https://doi.org/10.1016/j.dnarep.2019.02.005

66. Rape M. (2018). Ubiquitylation at the crossroads of development and disease. *Nature Reviews. Molecular Cell Biology*, *19*(1), 59–70. https://doi-org/10.1038/nrm.2017.83

67. Ronau, J. A., Beckmann, J. F., & Hochstrasser, M. (2016). Substrate specificity of the ubiquitin and Ubl proteases. *Cell Research*, *26*(4), 441–456. https://doi-org/10.1038/cr.2016.38

68. Rougé, L., Bainbridge, T. W., Kwok, M., Tong, R., Di Lello, P., Wertz, I. E., Maurer, T., Ernst, J. A., & Murray, J. (2016). Molecular Understanding of USP7 Substrate Recognition and C-Terminal Activation. *Structure (London, England: 1993)*, *24*(8), 1335–1345. https://doi-org/10.1016/j.str.2016.05.020

69. Saridakis, V., Sheng, Y., Sarkari, F., Holowaty, M. N., Shire, K., Nguyen, T., Zhang, R. G., Liao, J., Lee, W., Edwards, A. M., Arrowsmith, C. H., & Frappier, L. (2005). Structure of the p53 binding domain of HAUSP/USP7 bound to Epstein-Barr nuclear antigen 1 implications for EBV-mediated immortalization. *Molecular Cell*, *18*(1), 25–36. https://doi-org/10.1016/j.molcel.2005.02.029

70. Sarkari, F., La Delfa, A., Arrowsmith, C. H., Frappier, L., Sheng, Y., & Saridakis, V. (2010). Further insight into substrate recognition by USP7: structural and biochemical analysis of the HdmX and Hdm2 interactions with USP7. *Journal of Molecular Biology*, *402*(5), 825–837. https://doi-org/10.1016/j.jmb.2010.08.017

71. Sarkari, F., Wheaton, K., La Delfa, A., Mohamed, M., Shaikh, F., Khatun, R., Arrowsmith, C. H., Frappier, L., Saridakis, V., & Sheng, Y. (2013). Ubiquitin-specific protease 7 is a regulator of ubiquitin-conjugating enzyme UbE2E1. *The Journal of Biological Chemistry*, *288*(23), 16975–16985. https://doi-org/10.1074/jbc.M113.469262

72. Sheng, Y., Saridakis, V., Sarkari, F., Duan, S., Wu, T., Arrowsmith, C. H., & Frappier, L. (2006). Molecular recognition of p53 and MDM2 by USP7/HAUSP. *Nature Structural and Molecular Biology*, *13*(3), 285–291. https://doi.org/10.1038/nsmb1067

73. Sobhian, B., Shao, G., Lilli, D. R., Culhane, A. C., Moreau, L. A., Xia, B., Livingston, D. M., & Greenberg, R. A. (2007). RAP80 targets BRCA1 to specific ubiquitin structures at DNA damage sites. *Science (New York, N.Y.)*, *316*(5828), 1198–1202. https://doi-org/10.1126/science.1139516

74. Swatek, K. N., & Komander, D. (2016). Ubiquitin modifications. *Cell Research*, *26*(4), 399–422. https://doi-org/10.1038/cr.2016.39

75. Thrower, J. S., Hoffman, L., Rechsteiner, M., & Pickart, C. M. (2000). Recognition of the polyubiquitin proteolytic signal. *The EMBO journal*, *19*(1), 94–102. https://doi-org/10.1093/emboj/19.1.94

76. Valles, G. J., Bezsonova, I., Woodgate, R., & Ashton, N. W. (2020). USP7 Is a Master Regulator of Genome Stability. *Frontiers in Cell and Developmental Biology*, *8*, 717. https://doi-org/10.3389/fcell.2020.00717

77. Wang, I. C., Chen, Y. J., Hughes, D., Petrovic, V., Major, M. L., Park, H. J., Tan, Y., Ackerson, T., & Costa, R. H. (2005). Forkhead box M1 regulates the transcriptional network of genes essential for mitotic progression and genes encoding the SCF (Skp2-Cks1) ubiquitin ligase. *Molecular and Cellular Biology*, *25*(24), 10875–10894. https://doi-org /10.1128/MCB.25.24.10875-10894.2005

78. Wang, Y., Zhou, X., Xu, M., Weng, W., Zhang, Q., Yang, Y., Wei, P., & Du, X. (2016). OTUB1-catalyzed deubiquitination of FOXM1 facilitates tumor progression and predicts a poor prognosis in ovarian cancer. *Oncotarget*, *7*(24), 36681–36697. https://doi-org /10.18632/oncotarget.9160

79. Wang, Z., Kang, W., You, Y., Pang, J., Ren, H., Suo, Z., Liu, H., & Zheng, Y. (2019). USP7: Novel Drug Target in Cancer Therapy. *Frontiers in Pharmacology*, *10*, 427. https://doi-org/10.3389/fphar.2019.00427

80. Wilkinson K. D. (1997). Regulation of ubiquitin-dependent processes by deubiquitinating enzymes. *FASEB Journal: Official Publication of the Federation of American Societies for Experimental Biology*, *11*(14), 1245–1256. https://doi.org/10.1096/fasebj.11.14.9409543

81. Wonsey, D. R., & Follettie, M. T. (2005). Loss of the forkhead transcription factor FoxM1 causes centrosome amplification and mitotic catastrophe. *Cancer Research*, *65*(12), 5181–5189. https://doi-org /10.1158/0008-5472.CAN-04-4059

82. Zhang, N., Wei, P., Gong, A., Chiu, W. T., Lee, H. T., Colman, H., … Huang, S. (2011). FoxM1 Promotes β-Catenin Nuclear Localization and Controls Wnt Target-Gene Expression and Glioma Tumorigenesis. *Cancer Cell*, *20*(4), 427–442. https://doi.org/10.1016/j.ccr.2011.08.016

83. Zhang, X. Y., Varthi, M., Sykes, S. M., Phillips, C., Warzecha, C., Zhu, W., Wyce, A., Thorne, A. W., Berger, S. L., & McMahon, S. B. (2008). The putative cancer stem cell marker USP22 is a subunit of the human SAGA complex required for activated transcription and cell-cycle progression. *Molecular Cell*, *29*(1), 102–111. https://doi-org /10.1016/j.molcel.2007.12.015

84. Zhang, Z. M., Rothbart, S. B., Allison, D. F., Cai, Q., Harrison, J. S., Li, L., Wang, Y., Strahl, B. D., Wang, G. G., & Song, J. (2015). An Allosteric Interaction Links USP7 to Deubiquitination and Chromatin Targeting of UHRF1. *Cell Reports*, *12*(9), 1400–1406. https://doi-org/10.1016/j.celrep.2015.07.046

85. Zhu, Y., Gu, L., Lin, X., Cui, K., Liu, C., Lu, B., Zhou, F., Zhao, Q., Shen, H., & Li, Y. (2020). LINC00265 promotes colorectal tumorigenesis via ZMIZ2 and USP7-mediated stabilization of β-catenin. *Cell Death and Differentiation*, *27*(4), 1316–1327. https://doi-org/10.1038/s41418-019-0417-3